The mechanism of oxygen sensing and signal transduction in the heme-based oxygen sensor protein HemAT from *Bacillus subtilis*

Hideaki Yoshimura

2006

Contents

Chapter 1: General Introduction

Introduction

All of organisms and cells must sense and respond to various stimuli from their outer environment in order to survive and maintain their homeostasis. There are a wide variety of the stimuli, such as nutrients, harmful matters, pH, light, temperature, pressure, etc. Organisms and cells recognize these stimuli, and display some responses and/or adaptations for respective stimulus. To accept the respective stimulus, organisms and cells have various receptor (sensor) proteins.

In general, receptor proteins consist of several domains including a sensor domain and a functioning domain. The sensor domain senses the corresponding effector molecule or the external signal exclusively. The selectivity in the binding of the effector is achieved by the formation of multiple and specific interactions between the receptor protein and the effector molecules. When a receptor protein binds its cognate effector, a conformational alteration of the protein is induced by the interaction with the effector. As the result of transmission of the conformational alteration from the sensor domain to the functioning domain, the functioning domain expresses a respective role, such as enzymatic activity, transcriptional regulation, and controlling the activity of another enzyme.

In the case that the effector molecule is extremely small, the receptor protein must take a special strategy to recognize and discriminate the small effector molecule. It is difficult to form multiple and specific interactions between the effector and the receptor protein. Thus, the discrimination mechanism of small molecules by the cognate receptor protein is especially interesting subject to investigate.

Another interesting subject in the investigation on receptor proteins is the mechanism of signal transduction from the effector binding site to the functioning domain. Although there are a variety of structures in the sensor domain and the functioning domain depending on the effector molecules and the functions, the intramolecular signal transduction from the sensor domain to the

functioning domains is a crucial process for all receptor proteins to express their functions. Therefore, elucidating this signal transduction mechanism is very important to study the structure and function relationships of the receptor proteins.

In this work, the author chose an O_2 sensor protein HemAT from *Bacillus subtilis* to study the molecular mechanism of O_2 sensing and signal transduction. HemAT is a member of heme-based sensor proteins where a heme acts as the active site for sensing the effector molecule. In addition, HemAT functions as the aerotactic signal transducer, that is, HemAT controls the chemotaxis of *B. subtilis* toward O_2.

This thesis consists of four chapters. In Chapter 1, the general introduction is described. This chapter contains the background of this work and some properties of HemAT previously reported. In Chapter 2, the author describes the molecular mechanism of O_2 sensing by HemAT-Bs revealed by mutagenesis and spectroscopic studies including resonance Raman, EPR, and UV-Vis spectroscopies. In Chapter 3, the author describes the signal transduction mechanism of HemAT-Bs revealed by time-resolved resonance Raman spectroscopy. Finally, the summary of this work and the future prospects are presented in Chapter 4.

Heme-based CO and NO sensor proteins

While gas molecules are known to be the substrates and/or the products of several enzymatic reactions, a new physiological function of gas molecules have been found recently, in which some diatomic gas molecules function as physiological effector molecules to regulate various biological functions in many organisms. Oxygen (O_2), carbon monoxide (CO), and nitric oxide (NO) are the typical gas molecules functioning as signaling molecules.

O_2, CO, and NO cannot be bound to protein directly. The sensor proteins for these gas molecules must therefore have a cofactor that functions as the binding site of these gas molecules. Many gas sensor proteins utilize a heme as the binding site of the effector gas molecule. Typical

heme-based gas sensor proteins are summarized in Table 1. Heme is a complex of an iron ion and a protoporphyrin (Figure 1). In most of heme proteins, one or two amino acids are coordinated to the heme iron as the axial ligands. The axial ligand tethers the heme to the protein matrix. In addition to this coordination, the high hydrophobicity of the porphyrin plane helps the heme to stay in the protein matrix stably. The cytoplasm in a cell is usually in reducing conditions, which usually keeps the heme iron in heme proteins in the Fe(II) state (ferrous state). The Fe(II) heme (ferrous state) can bind O_2, CO and NO reversibly. These properties of a heme are convenient for gas sensor proteins to utilize a heme as the binding site of the gas molecule. On the other hand, these gas molecules are difficult to form multiple and specific interactions with the protein matrix of the corresponding receptor proteins because of their small sizes. Moreover, a ferrous heme binds all of O_2, CO, and NO equally. These features of a heme make the selective molecular recognition difficult. As described above, a sensor protein must discriminate its cognate effector molecule with high specificity. If this discrimination is absent, the receptor protein will lose its functions and/or be out of control. To avoid the disruption of selectivity, heme-based gas sensor proteins adopt a unique mechanism for selective gas sensing, which will be discussed in the following sections.

Table 1. Typical heme-based gas sensor proteins

Protein	effector	function
CooA	CO	Transcriptional regulator
sGC	NO	Enzyme to form cGMP from GTP
FixL	O_2	Sensor kinase of the FixL/FixJ two-compornent signal transduction system
HemAT	O_2	Aerotactic signal transducer
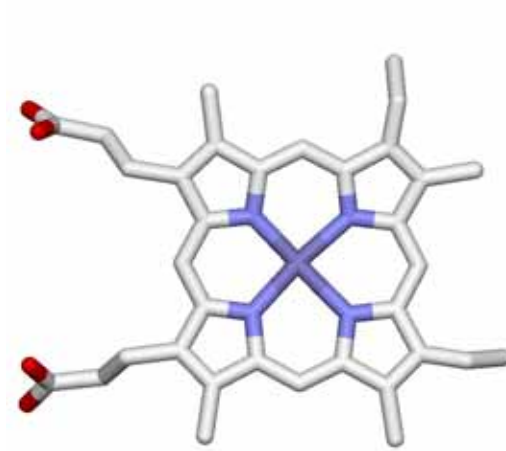
Figure 1. The molecular structure of heme.

CO sensor protein CooA

CooA is a typical heme-based CO sensor protein that functions as a transcriptional regulator in CO metabolizing bacteria. CooA activates the expression of the proteins required for the CO metabolism including CO dehydrogenase and hydrogenease in the presence of CO under anaerobic condition.[1] Only CO-bound CooA can bind to the target DNA to act as a transcriptional activator, but the ferric and ferrous CooA cannot. A conformational change is induced by the CO binding to the heme in CooA, which is the trigger of the activation of CooA by CO. The mechanism of CO sensing has been extensively studied for CooA from *Rhodospirillum rubrum* (Rr-CooA) and *Carboxydothermus hydrogenoformans* (Ch-CooA).

Rr-CooA and Ch-CooA contain a *b*-type heme (protoheme) as the active site for sensing CO. The heme in Rr-CooA has two axial ligands, (Pro[2] and Cys[75]) and (Pro[2] and His[77]) for the ferric and ferrous hemes, respectively. Pro[2] is the N-terminal residue because Met[1] is removed by post-translational modification. When ferrous CooA reacts with CO, Pro[2] is replaced by CO to form CO-bound CooA.

Ch-CooA also has a 6-coordinated heme in the ferric, ferrous, and CO-bound forms, but its coordination structure is slightly different from that of Rr-CooA. While the ligand exchange takes place between Cys^{75} and His^{77} upon the change in the oxidation state of the heme in Rr-CooA, such a ligand exchange does not occur in Ch-CooA. In Ch-CooA, the N-terminal α-amino group is coordinated to the ferric and ferrous hemes as the distal 6th ligand. The α-amino group coordinated to the ferrous heme is replaced by CO upon the CO binding to the heme in Ch-CooA.

Although the N-terminal amino acid residue is not conserved between Rr-CooA and Ch-CooA, the coordination of the N-terminus, the N-terminal Pro and α-amino group in Rr-CooA and Ch-CooA, respectively, is conserved between them. The more important property conserved between Rr-CooA and Ch-CooA is that the N-terminus coordinated to the ferrous heme is replaced by CO upon the CO binding. The dissociation of the N-terminus from the heme takes place upon the CO binding. The dissociation of the N-terminus from the heme upon the CO binding will induce a conformational change around the heme, which is a trigger of the activation of CooA by CO.

When ferrous CooA reacts with O_2, a rapid autoxidation proceeds to form the ferric form without the formation of a stable O_2-bound form. As described above, ferric CooA is an inactive form disable to binding to the target DNA. Therefore, O_2 cannot activate CooA.

NO also cannot activate Rr-CooA, though NO can bind to the heme in Rr-CooA. When Rr-CooA reacts with NO, a 5-coordinated nitrosyl heme is formed, where all of the endogenous axial ligands are dissociated from the heme. The dissociation of the proximal His upon the NO binding will result in the different conformation of NO-bound Rr-CooA compared with CO-bound CooA, because the proximal His is retained in CO-bound CooA. In the case of Ch-CooA, the dissociation of proximal His does not occur upon NO binding. As the result, Ch-CooA exhibits some activity upon the NO binding. Thus, the dissociation of proximal His in Rr-CooA is essential for the discrimination between CO and NO.
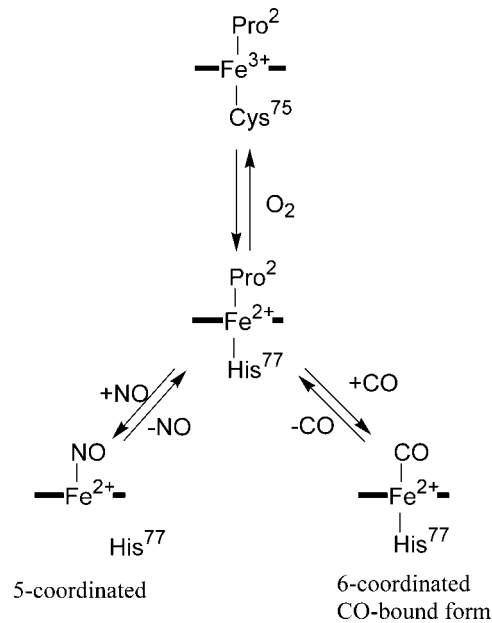
$$\text{Pro}^2$$
$$| $$
$$-\text{Fe}^{3+}-$$
$$| $$
$$\text{Cys}^{75}$$

$$\updownarrow \quad O_2$$

$$\text{Pro}^2$$
$$| $$
$$-\text{Fe}^{2+}-$$
$$| $$
$$\text{His}^{77}$$

+NO ⤢ -NO   -CO ⤡ +CO

5-coordinated:
$$\text{NO}$$
$$| $$
$$-\text{Fe}^{2+}-$$
$$| $$
$$\text{His}^{77}$$

6-coordinated CO-bound form:
$$\text{CO}$$
$$| $$
$$-\text{Fe}^{2+}-$$
$$| $$
$$\text{His}^{77}$$

5-coordinated

6-coordinated
CO-bound form

Figure 2. The coordination structures of the heme in Rr-CooA. Pro[2] is the N-terminal residue because Met[1] is removed by post-translational modification.

NO sensor protein sGC

sGC from mammal is a typical NO sensor protein, which catalyze the formation of cGMP from GTP.[2] The enzymatic product, cGMP, functions as a second messenger that controls various function of the mammal. The enzymatic activity of sGC is activated by NO binding to the heme in sGC by 200~300 fold. The alteration in the coordination structure of the heme in sGC upon CO and NO binding is similar to that of CooA. In ferrous state without external ligands, the heme in sGC takes a 5-coordinated structure with a histidine as an axial ligand. Upon CO binding to the heme, the heme takes a 6-coordinated structure with His and CO as the axial ligands. However, the activity of sGC is enhanced only by 4~5 fold upon CO binding. As described above, NO activates sGC by 200~300 fold. These differences result from the difference of the coordination structure of the heme in CO- and NO-bound forms. When NO binds to the heme in sGC, the dissociation of the Fe—His bond takes place to form a 5-coordinated nitrosyl heme. This dissociation of the Fe—His bond will

induce a conformational change of sGC to be a trigger of the activation of sGC by NO. Because the dissociation of the Fe—His bond does not occur upon the CO binding, CO cannot activate sGC as does NO. Thus, sGC discriminates CO from NO by the different coordination structure.

O$_2$ is not bound to the heme in sGC even in the environment with O$_2$ because of low affinity of O$_2$ to the heme. Although the detail mechanism of this low O$_2$ affinity is not clear, sGC discriminates O$_2$ from NO by the different binding affinity.
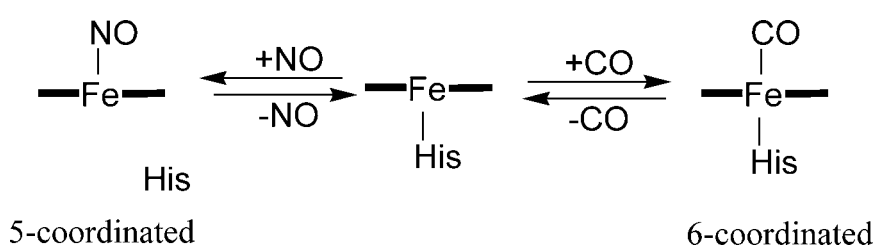

Figure 3. The coordination structure of the heme in sGC.

Heme-based O$_2$ sensor proteins

Aerobes require O$_2$ to obtain the energy for growth by aerobic respiration where O$_2$ functions as the final electron acceptor in the electron transport chain. Moreover, O$_2$ is necessary for oxidation reaction by oxidases and oxygenases such as P450s, tyrosinase, and catechol dioxygenase. Thus O$_2$ is one of the essential substrates for many organisms to maintain their lives. On the other hand, excess O$_2$ sometimes behaves as a harmful matter in biological systems by the formation of reactive oxygen species. Organisms must therefore sense the suitable O$_2$ concentration and make an exact response and adaptation. Some bacteria sense the O$_2$ concentration, and exhibit a chemotactic response toward or against O$_2$, which called aerotaxis. In the case of mammal, hypoxic condition of the cell stabilizes hypoxia inducible factor 1α (HIF1α) that is a transcriptional regulator inducing the expression of genes required for the response to hypoxia[3]. The stability of HIF1α is controlled whether it is hydroxylated or not. Proline hydroxylase catalyzes the hydroxylation of HIF1α with O$_2$

under aerobic condition, but the hydroxylation is stopped by hypoxia. Thus proline hydroxilase acts as an O_2 sensor in this system.

However, for selective O_2 sensing, heme-based O_2 sensor proteins must have peculiar mechanism in different manner from that in CO and NO sensor proteins. CO and NO sensor proteins utilize the lower affinity of O_2 to the heme. This feature of O_2 is, however, just a disadvantage to O_2 sensing and discrimination. Heme-based O_2 sensor proteins cannot take a ligand discrimination strategy by exclusive binding of O_2. In fact, the affinity of CO to heme without protein matrix is reported 27,000 times larger than that of O_2[4]. Even in myoglobin, in which the affinity for O_2 is increased by hydrogen bond formation between the heme-bound O_2 and a histidine residue in the heme distal pocket, and that for CO is remarkably decreased by a static hindrance by amino acid, the affinity of CO is still 25 times higher than that of O_2[5]. In general the affinity of NO to the heme is still higher than that of CO. These facts suggest that heme-based O_2 sensor proteins cannot avoid the binding of CO and NO. Therefore, heme-based O_2 sensor proteins, must equip special mechanisms for selective O_2 sensing. These mechanisms have not been fully understood yet, but partially elucidated in some O_2 sensor proteins.

O_2 sensor protein FixL

FixL is a sensor kinase of the FixL/FixJ two-component system that regulates the expression of *nif* genes responsible for N_2 fixation in rhizobia.[6] The kinase activity of FixL is regulated by O_2, in which FixL senses O_2 by means of a heme. When O_2 is bound to the heme in FixL, the kinase activity of FixL is inhibited. Once O_2 is dissociated from the heme, FixL is activated as the kinase to carry out the autophosphorylation and then the phosphoryl transfer to FixJ.

The crystal structures of FixL from different sources have been solved in various forms, providing much information to consider the mechanism of selective O_2 recognition. The crystal structures of FixL from *Bradyrhizobium japonicuum* (BjFixL) are shown in Figure 4 for the deoxy O_2-, CO-, and NO-bound forms. In the case of BjFixL, Arg220 forms a hydrogen bond to the heme propionate 7 in the ferrous deoxy state. This hydrogen bond is present in CO- and NO-bound forms. Only in the O_2-bound form, the hydrogen bond between Arg220 and the heme propionate 7 is broken,

resulting in the movement of Arg220 into the heme distal pocket where the heme-bound O_2 is present. And then Arg220 forms a hydrogen bond to the heme-bound O_2. This specific hydrogen-bonding pattern in the O_2-bound form is considered to be essential for the O_2 discrimination by FixL.

The movement of the FG-loop where Arg220 is located will be induced by the reconstruction of the hydrogen bonding network triggered by O_2 binding, which may induce the structural change responsible for kinase inactivation. Though CO and NO bind to the distal position of the heme as does O_2, they do not induce the reconstruction of the hydrogen bonding network in the distal heme pocket. These results are consistent with the fact that CO and NO are weak inhibitors for FixL while O_2 is a strong one.
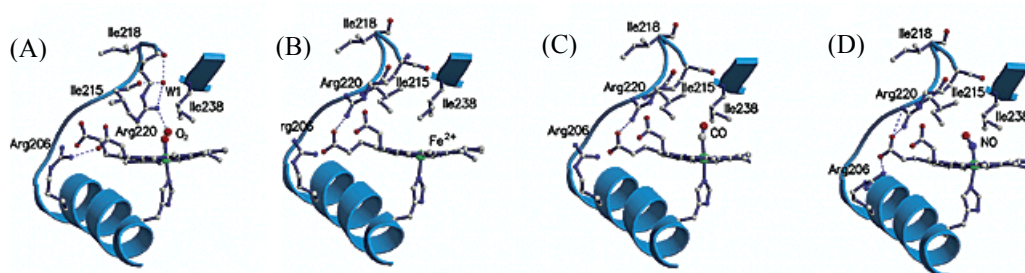
Figure 4. The reported crystal structures of FixL from Bradyrhizobium japonicum in the (A) O_2-bound, (B) frerrous, (C) CO-bound, and (D) NO bound forms[7]. Arg220 forms a hydrogen bond to the heme-bound ligand only in the O_2-bound form. This specific hydrogen bond formation would essential for the selective O_2 sensing and induce the signaling event.

The heme-based aerotactic signal transducer HemAT

HemAT is a heme-based O_2 sensor protein responsible for the aerotaxis control in some bacteria. While the putative gene of HemAT has been reported in tens of bacteria so far,[8] just a few HemAT are confirmed to function as the aerotactic signal transducer. *B. subtilis* is one of such bacteria containing HemAT as an aerotactic signal transducer.

In 1997, the whole genome analysis of *B. subtilis* has been completed, and 10 putative genes

were identified as chemotactic signal transducer proteins. [9] Alam and co-workers found that the N-terminal region in the one of these proteins, YhfV, displays a limited homology to myoglobin (Mb), and named it HemAT-Bs.[10] The amino acid sequence of Mb and HemAT-Bs are shown in Figure 5. The recombinant HemAT-Bs expressed in *Escherichia coli* (*E. coli*) contains a heme and shows similar UV/Vis spectra to Mb. While the aerotactic response was lost in the *B. subtilis* Δten strain where all of the putative 10 chemotactic signal transducer proteins were deleted, the expression of HemAT-Bs in the Δten strain rescued the aerophilic response of this bacterium. These results clearly show the function of HemAT-Bs as the aerotactic signal transducer protein.

HemAT-Bs consists of two domains: the N-terminal sensor domain (residues 1-178) and the C-terminal signaling domain (residues 198-432). Phillips and co-worker reported the crystal structure of the sensor domain (Figure 6B).[11] The sensor domain of HemAT-Bs indeed shows a globin fold similar to that of Mb (Figure 6). The crystal structure of the sensor domain of HemAT-Bs reveals that the homology alignment of HemAT-Bs and Mb previously presented by Alam and co-workers is considerably different from the actual structural alignment. A few difference of the structural feature of HemAT-Bs and Mb is observed. HemAT-Bs lacks the D helix, and an extra helix is present in the N-terminal, named the Z helix. Phe69 and Tyr70 are present in the B helix in HemAT-Bs, which are not present in Mb and mammalian Hb, but are highly conserved in Hb from some bacteria, plant, and protozoa. In addition, HemAT-Bs has no distal histidine residue that stabilizes the heme-bound O_2 in the case of Mb and Hb (Figure 7,8). These facts indicate that HemAT-Bs will belong to the ancient globin family rather than the globins from higher animals.
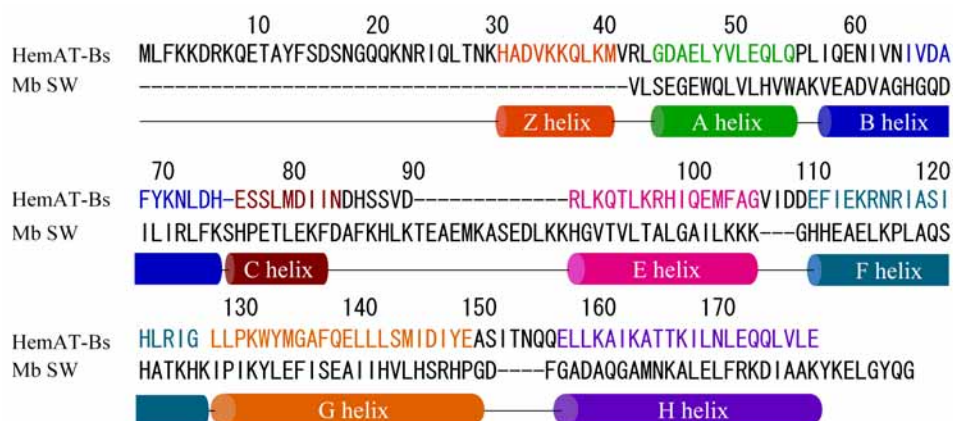
Figure 5. The amino acid sequences of the sensor domain in HemAT and sperm whale Mb.

Among the heme-based O_2 sensor proteins, HemAT-Bs is the first discovered globin-coupled sensor protein. The investigation about HemAT may, therefore, give a novel mechanism of selective O_2 sensing. Moreover, we may be able to reveal the essential factor for selective O_2 sensing with comparing the mechanisms of HemAT-Bs and those of other heme-based O_2 sensor proteins.

As mentioned above, heme-based O_2 sensor proteins must discriminate O_2 from other small molecules, such as CO and NO. However, it is hard for heme proteins to discriminate O_2 among these molecules, because all of these molecules have an almost similar shape and size. Though O_2, CO and NO can bind to a heme, the affinity of these molecules to a heme is different. CO and NO show higher affinity than O_2 does. Because of this difference of affinity, some heme-based CO and NO sensor proteins such as CooA and sGC can avoid the binding of O_2 to their heme to discriminate their effector from O_2. This lower affinity of O_2 to the heme, however, is unfavorable for heme-based O_2 sensor proteins to sense O_2 selectively. In principle, all of O_2, CO, and NO are bound to the heme in the heme-based O_2 sensor proteins. Thus, heme-based O_2 sensor proteins must adopt a special mechanism for selective O_2 recognition.
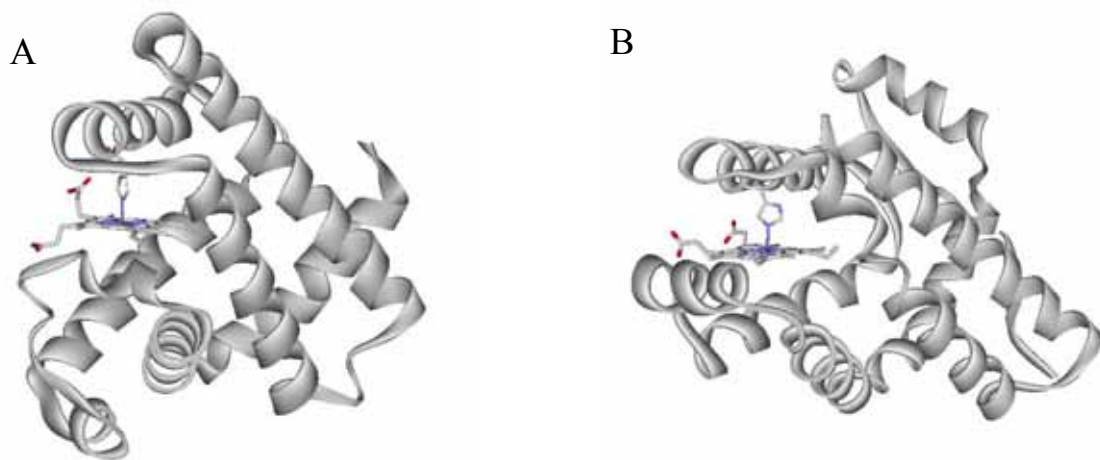
Figure 6. The crystal structure of (A) myoglobin and (B) the A subunit of HemAT sensor domain.
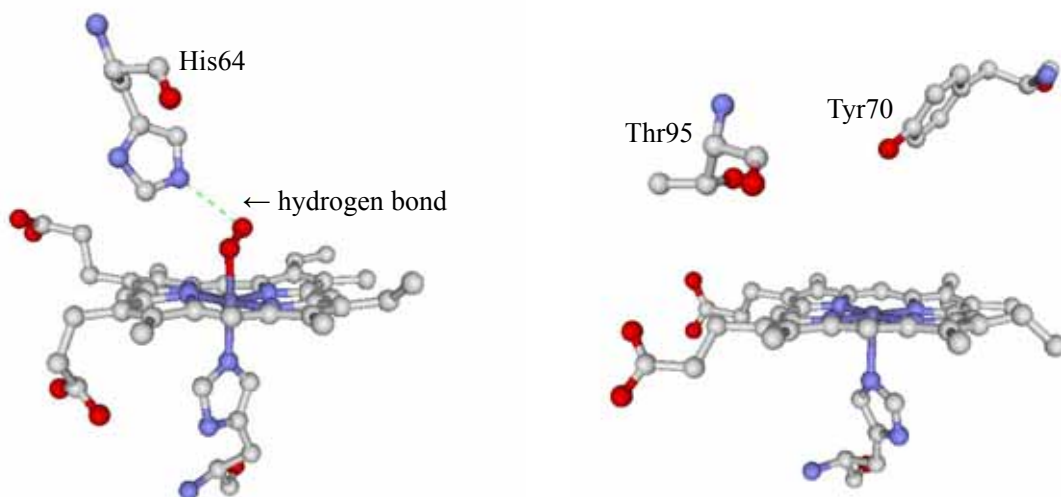

Figure 7. The crystal structure around the heme in (A) O_2-bound myoglobin and (B) the A subunit of deoxy HemAT-Bs
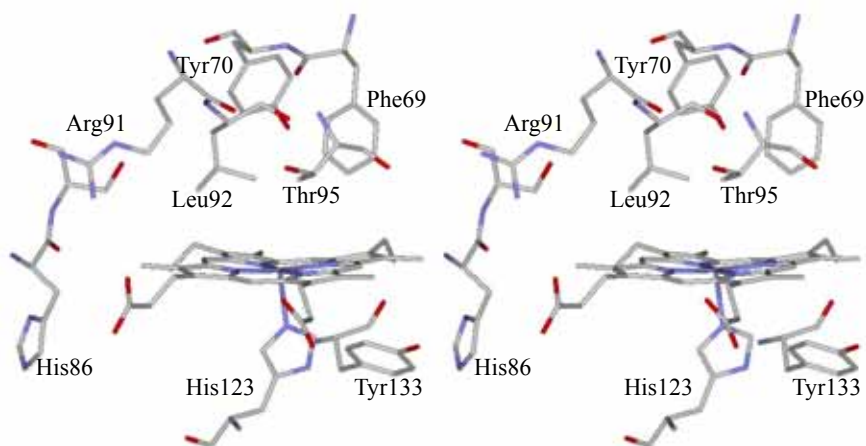
Figure 8. The stereo view of the crystal structure around the heme in the subunit A of ferrous HemAT-Bs (PDB: 1OR6).

The protein structure of the sensor domain, especially the heme distal structure, would be important to achieve the selective O_2 sensing by the heme-based O_2 sensor proteins because only the amino acid residues in the distal heme pocket can interact to the heme-bound O_2. As described above, investigations on the heme-based O_2 sensor protein FixL gives an example of the specific interaction between the heme-bound O_2 and an amino acid residue in the distal heme pocket.

The distal heme pocket in HemAT-Bs includes two polar amino acid residues, Tyr70 in the B helix and Thr95 in the E helix (Figure 8). Resonance Raman spectroscopy has shown that there are three conformers with different hydrogen bonding pattern to the heme-bound O_2 (Figure 9):[12] a conformer with hydrogen bonds from Thr95 to both of the O atoms of the heme-bound O_2 via a water molecule (closed form), a conformer with a direct hydrogen bond from Thr95 to the proximal O atom of the heme-bound O_2 (open α form), and a conformer without hydrogen bonds to the heme-bound O_2 (open β form). Thus, the hydrogen bond between the heme bound O_2 and Thr95 would be responsible for the selective O_2 recognition and signal generation. However, the O_2 discrimination mechanism of HemAT-Bs is not obvious.
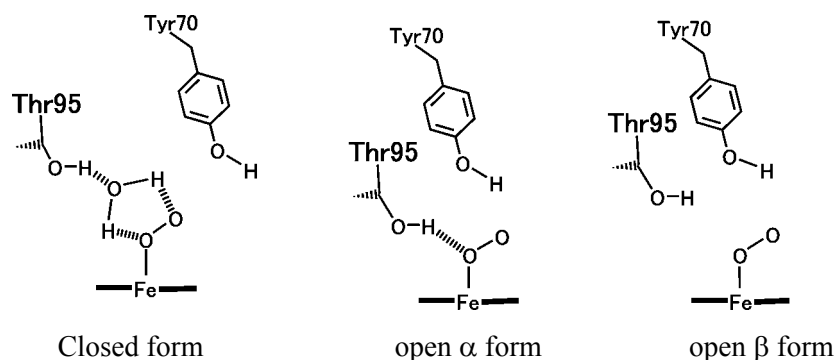
17

Figure 9. The three conformations of the O_2-bound HemAT-Bs

Chemotaxis signal transduction system in bacteria

HemAT-Bs is a signal transducer protein in aerotaxis (chemotaxis toward O_2) control system in *B. subtilis*. In this section, a background of the chemotaxis system in bacteria is described. Most of bacteria exhibit chemotactic responses when the bacteria sense attractants or repellents. In general, one bacterium has several chemotactic sensor proteins to sense various effectors for chemotaxis. The most typical proteins for chemotactic receptor are methyl-accepting chemotaxis proteins (MCPs), which are generally transmembrane proteins consisting of the sensor domain in the periplasm and the signaling domain in the cytoplasm.[13] The amino acid sequence of the HemAT signaling domain exhibits high homology to other MCP signaling domains despite of that HemAT is a soluble protein. The amino acid sequence of the signaling domain is 30% identical to the signaling domain of Tsr from *E. coli*, a typical bacterial chemotactic receptor protein called methyl-accepting chemotaxis protein (MCP). Therefore HemAT-Bs can be considered as a member of MCPs.

The chemotaxis control system consists of MCP, CheW, CheA and CheY (Figure 7).[13] When an effector molecule is bound to the sensor domain of the MCP, a structural alteration of the sensor domain induced by the effector binding is transmitted to the signaling domain. The structural alteration of MCP regulates the activity of the histidine kinase protein CheA through the adaptor

protein CheW. CheW is necessary for the signal transduction from MCP to CheA, although CheW is not required to form the complex between MCP and CheA. In the most bacteria including *E. coli*, the CheA activity is down regulated, that is, CheA activity is "on" state without the binding of the effector molecule to the MCP sensor domain, while the binding of the effector to MCP turn off the kinase activity of CheA. On the other hand, some bacteria, for example *B. subtilis*, exhibit the opposite system of the CheA regulation; the binding of the effector to MCP activates the CheA kinase. The phosphate group on the activated CheA is transmitted to CheY, a response regulator. And then, the phosphorylated CheY interacts with the flagellar motor to control the direction of the flagellar motor rotation.
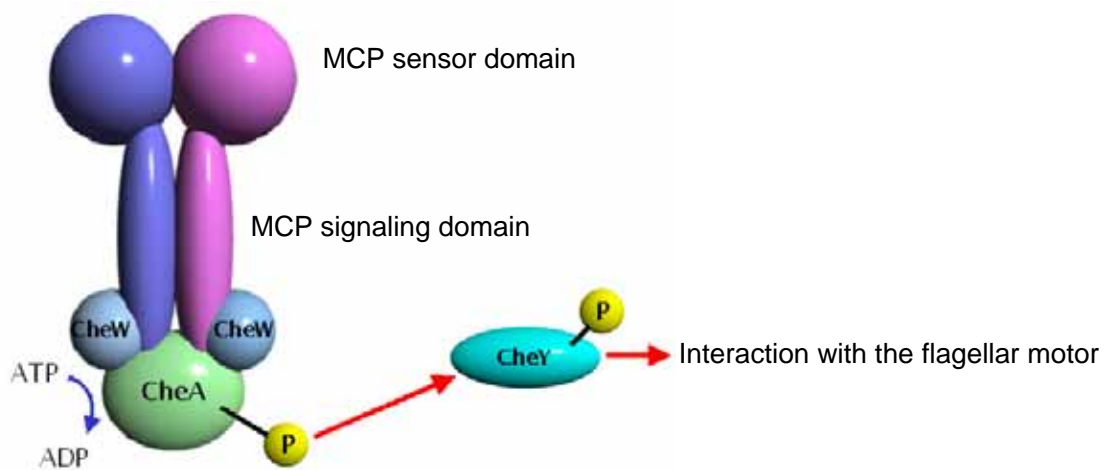
Figure 9. A schematic model of the aerotactic signaling system with MCP, CheW, CheA, and CheY.

The amino acid sequences of the MCP signaling domains show substantial homology (Figure 10), and the signaling domain can be considered to have a conserved structure regardless of the effectors. The crystal structure of the signaling domain of the serine receptor from *E. coli* (Tsr) and another MCP from *Thermotoga maritima* are solved by X-ray crystallography.[14,15] As shown in Figure 8B, the MCP signaling domain forms a dimer that constructs a huge four-helix-bundle with

about the length of 200 Å and the diameter of 20 Å. Each subunit contributes two helices with a U-turn tip, where the amino acid sequence is especially conserved. The tip would be the interface to CheW and CheA.

A

```
Tsr      216 --------ASLVAPMNRLIDSIRHIAGGDLVKPIEVDGSNEMGQLAESLRHMQGELMRTVG 268
McpB     297 ILILFIVRSITKPLKRLVQSSKTISRGDLTETIEIHSKDELGELGESFNEMGQSLRSLIS 356
HemAT-Bs 179 ---------------------------------AFQSEYNQTRDEQEEKKNLLHQKIQETSG 207

Tsr      269 DVRNGANAIYSGASEIATGNNDLSSRT--------------EQQAASLEETAASMEQLTA 314
McpB     357 AIQNSVNNVAASSEQLTASAGQTSKATEHITMAIEQFSNGNEEQSRKVESSSHQLNLMNE 416
HemAT-Bs 208 SIANLFSETSRSVQELV------------------------DKSEGISQASKAGTVTSS 242

Tsr      315 TVKQNAENARQASHLALSASETAQRGGKVVDNVVQTMRDISTSSQK------------- 360
McpB     417 GLQQVSQTSSDITKASIQSTEIAGTGEKFVQQTGGQMNSINQSVQQAEAVVKGLEGKSKD 476
HemAT-Bs 243 TVEEKSIGGKK--ELEVQQKQMNKIDTSLV-QIEKEMVKLDEIAQQ------------- 285

Tsr      361 IADIISVIDGIAFQTNILALNAAVEAARAGEQGRGFAVVAGEVRNLAQRSAQAAREIKSL 420
McpB     477 ITSILRVINGIADQTNLLALNAAIEAARAGESGRGFSVVAEEVRKLAVQSADSAKEIEKL 536
HemAT-Bs 286 IEKIFGIVTGIAEQTNLLSLNASIESARAGEHGKGFAVVANEVRKLSEDTKKTVSTVSEL 345

Tsr      421 IEDSVGKVDV--------------GSTLVESAGETMAEIVSAVTRVTDIMGEIASASDEQ 466
McpB     537 IQEIVAEIDTSLHMFKEVNQEVQSGLVVTDNTKESFQSIFSMTNEIAGKLQTMNSTVEQL 596
HemAT-Bs 346 VNNTNTQINI-------------------VSKHIKDVNELVSESKEKMTQINRLFDE- 383

Tsr      467 SRGIDQVGLAVAEMDRVTQQNAALVEESAAAAAALEEQASRLTEAVAVFRIQQQQRETSA 526
McpB     597 SDRSQHVSAAVSGIADVSKESSASIQDIAASA----EEQLASMEE----------------- 637
HemAT-Bs 384 -----------IVHSMKISKEQSGKIDVDLQAF-------LGGLQE----------------- 411

Tsr      527 VVKTVTPAAPRKMAVADSEENWETF 551
McpB     638 ISSSATTLAQMAEELRDLTKQFKIE 662
HemAT-Bs 412 VSRAVSHVAASVDSLVILTEE---- 432
```

B

Figure 10. (A) Amino acid sequence alignment in the signaling domain of Tsr from *E. coli,* McpB from *B. subtilis*, and HemAT-Bs. (B) the reported crystal structure of the signaling domain of MCP from *Thermotoga maritina* (PDB: 2CH7).

The periplasmic sensor domain and the cytoplasmic signaling domain of MCP are connected by the transmembrane domain. The movement of the transmembrane region should be important for the signal transduction from the sensor domain to the signaling domain. This region consists of helices called TM1 and TM2, which form a helix-bundle motif. In the most cases, TM1 and TM2 are the N and the C terminal helices of the sensor domain, respectively. TM2 is connecting with the extended helix of the signaling domain. Koshland and co-worker estimated the movement of the

transmembrane region of *E. coli* aspartate receptor, Tsr, using a site-directed spin-labeling method.[16] They conclude that the helix bundle of the transmembrane region exhibits an about 1 Å "piston-like movement" (Figure 11). On the other hand, Ordal and co-worker performed a disulfide crosslinking study on the aspartate receptor, McpB, from *B. subtilis*, and showed a rotational movement on the TM1 (Figure 11).[17] The similar helix bundle motif is observed not only in MCPs but also in many other receptor proteins. It is not determined at present which model is correct for signal transduction. There are some reports that chimera proteins consisting of MCP sensor domain and the signaling domain of another receptor protein retain the signaling ability. Therefore, the information from the investigation about MCP would useful to resolve the general mechanism of receptor proteins.
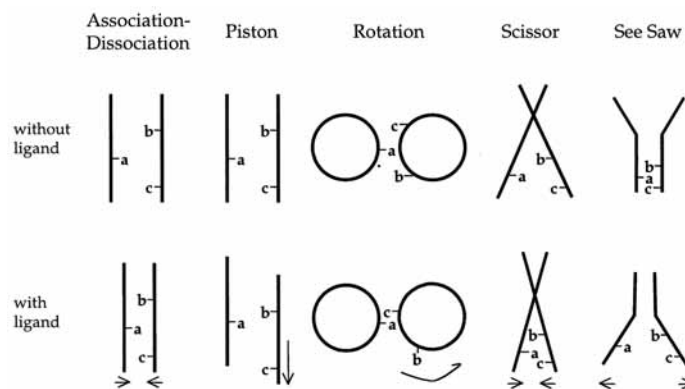

Figure 11. The models for the patterns of conformational alteration in a helix bundle by Koshland et al.[16]

The purpose of this work

Since HemAT belongs to the MCP family, the conformational change of HemAT upon O_2 binding would be in the same pattern to other MCP proteins. Although the movement of the region between the sensor and signaling domain is proposed for the intramolecular signal transduction for MCP, the detail mechanism is not clear yet. Among MCPs, HemAT is an excellent model for investigation of MCP because HemAT-Bs is the only soluble protein among MCPs so far isolated. Moreover, HemAT-Bs has a heme, which is a good probe for several spectroscopic studies. These features would also help the investigation especially about the mechanism of signal transduction upon effector binding.

There are two purposes in this work on HemAT-Bs. One is the elucidation of the mechanism of the selective O_2 sensing, and the other is the elucidation of the intramolecular signal transduction mechanism. To elucidate these mechanisms, the author has done the mutagenesis and spectroscopic studies on HemAT-Bs

REFERENCES

1. Aono, S (2003) Biochemical and biophysical properties of the CO-sensing transcriptional activator CooA, *Acc. Chem. Res. 36*, 825-831

2. Pal, B. and Kitagawa, T. (2005) Interactions of soluble guanylate cyclase with diatomics as probed by resonance Raman spectroscopy, *J. Inorg. Biochem.*, *99*, 267-279

3. Berra, E., Ginouves, A. and Pouyssegui, J. (2006) The hypoxia-inducible-factor hydroxylases bring fresh air into hypoxia signalling, *EMBO Rep.*, *7*, 41-45

4. Traylor, T. G., Mitchell, M. J., Tsuchiya, S., Campbell, D. H., Stynes D. V. and Koga, N. (1981) Cyclophane hemes. 4. Steric effects on dioxygen and carbon monoxide binding to hemes and

heme proteins, *J. Am. Chem. Soc. 103*, 5234-5236

5.   Olson, J. S. and Phillips, G. N. Jr. (1997) Myoglobin discriminates between O2, NO, and CO by electrostatic interactions with the bound ligand, *J.Biol. Inorg. Chem.*, *2*, 544-552

6.   Chan, M. K. (2001) Recent advances in heme-protein sensors, *Curr. Opin. Chem. Res. 5*, 216-222

7.   Hao, B., Isaza, C., Arndt, J., Soltis, M. and Chan, M. K. (2002) Structure-based mechanism of O_2 sensing and ligand discrimination by the FixL heme domain of *Bradyrhizobium japonicum*, *J. Am. Chem. Soc. 126*, 15000-15001

8.   Allen, T., Freitas, K. and Alam, M. (2003) The diversity of globin-coupled sensors, *FEBS Lett.*, *552*, 99-104

9.   Kunst, F. *et al*. (1997) The complete genome sequence of the gram-positive bacterium *Bacillus subtilis*, *Nature 309*, 249-256

10.   Hou, S., Larsen, R. W., Boudko, F., Riley, C. W., Karatan, E., Zimmer, M., Ordal, G. W. and Alam, M. (2000) Myoglobin-like aerotaxis transducers in Archaea and Bacteria, *Nature 403*, 540-544

11.   Zhang, W. and Phillips, G. N. Jr. (2003) Structure of the oxygen sensor in *Bacillus subtilis*: signal transduction of chemotaxis by control of symmetry, *Structure 11*, 1097-1110

12.   Ohta, T., Yoshimura, H., Yoshioka, S., Aono, S. and Kitagawa, T. (2004) Oxygen-sensing mechanism of HemAT from *Bacillus subtilis*: A resonance Raman spectroscopic study, *J. Am. Chem. Soc. 126*, 15000-15001

13.   Szurmant, H. and Ordal, G. W. (2004) Diversity in chemotaxis mechanisms among the bacteria and archaea, *Microbiol. Mol. Biol. Rev. 68*, 301-319

14.   Kim, K. K., Yokota, H. and Kim, S. H. (2000) Four-helix bundle structure of the cytoplasmic domain of a serine chemotaxis receptor, *Nature 400*, 787-792

15.   Park, S. Y., Borbad, P. P., Gonzalez-Bonet, G., Bhatnager, J., Pollard, A. M., Freed, J. H., Bilwes, A. M. and Crane, B. R. (2006) Reconstruction of the chemotaxis receptor-kinase assembly, *Nat.*

Struct. Mol. Biol 13, 400-407

16.   Ottemann, K. M., Xiao, W., Shin, Y. and Koshland, D. E. Jr. (1999) A piston model for transmembrane signaling of the aspartate receptor, *Science*, *285*, 1751-1754

17.   Szurmant, H., Bunn, M. W., Cho, S. H. and Ordal, G. W. (2004) Ligand-induced conformational changes in the *Bacillus subtilis* chemoreceptor McpB determined by disulfide crosslinking *in vivo*, *J. Mol. Biol.*, *344*, 919-928

Chapter 2: Specific hydrogen-bonding networks responsible for selective O$_2$ sensing of HemAT-Bs

Abstract

HemAT-Bs discriminates its physiological effector, O$_2$, from other gas molecules to generate the aerotactic signal, but the detailed mechanism of the selective O$_2$ sensing is not obvious. In this study, the author measured electronic absorption, electron paramagnetic resonance (EPR), and resonance Raman spectra of HemAT-Bs to elucidate the mechanism of the selective O$_2$ sensing by HemAT-Bs. The resonance Raman spectroscopy revealed that a hydrogen bond is formed between His86 and the heme propionate only in the O$_2$-bound form, in addition to that between Thr95 and the heme-bound O$_2$. Disruption of this hydrogen bond by the mutation of His86 caused disappearance of a conformer with a direct hydrogen bond between Thr95 and the heme-bound O$_2$ that is present in WT HemAT-Bs. On the basis of these results, the author proposes a model for the selective O$_2$ sensing by HemAT-Bs as follows. The formation of the hydrogen bond between His86 and the heme propionate induces a conformational change of the CE-loop and the E-helix, by which Thr95 is located at the proper position to form the hydrogen bond with the heme-bound O$_2$. This stepwise conformational change would be essential to the selective O$_2$ sensing and the signal transduction by HemAT-Bs.

Introduction

The diatomic gas molecules such as dioxygen (O_2), carbon monoxide (CO), and nitric oxide (NO) can work as signaling molecules with the cognate receptor proteins in biological systems. The heme-based sensor proteins are the most general receptor proteins for these gas molecules.[1-3] The heme in these proteins functions as the binding site for the effector gas molecules. These heme-based gas sensor proteins must discriminate the effector from other molecules so as to take a specific conformation only upon the binding of the effector molecule. However, the discrimination of these gas molecules is difficult for heme proteins because all of O_2, CO, and NO have similar size and can be bound to a reduced heme with a similar coordination structure. The ligand discrimination mechanism of the heme-based gas sensor proteins is not fully understood yet.

HemAT is a heme-based O_2 sensor protein that functions as a signal transducer for bacterial aerotaxis.[4-7] HemAT monomer consists of two domains, a sensor domain and a signaling domain. The sensor domain shows a globin fold containing a heme that acts as the O_2 binding site. The signaling domain of HemAT interacts with a histidine kinase protein CheA, a component of the CheA/CheY two-component signal transduction system that regulates the direction of the flagellar motor rotation.[8-10]

A specific conformational change of HemAT will occur around the heme upon O_2 binding, and then intramolecular signal transduction takes place from the sensor domain to the signaling domain. As a result, the self-kinase activity of CheA is regulated by a change in the HemAT-CheA interaction via the conformational change of HemAT. This signaling event takes place only with O_2, but not with other gas molecules. However, the detailed mechanisms of the selective O_2 sensing and the signal transduction of HemAT remain to be elucidated.

To elucidate these mechanisms of HemAT, it is necessary to characterize the heme environmental structure including the coordination structure of the heme and hydrogen-bonding pattern around the heme and the ligand. The crystal structure of the sensor domain of HemAT from *Bacillus subtilis* (HemAT-Bs) reveals that Tyr70 and Thr95 in the distal heme pocket are possible candidates of amino acid residues to form hydrogen bonds with the heme-bound ligand (Figure 1).[11]

Resonance Raman spectroscopy has revealed that Thr95 forms hydrogen bonds to the heme-bound O_2, but Tyr70 does not.[12] Oxygen-bound HemAT-Bs has three different conformers with different hydrogen bonding pattern around the heme-bound O_2. The hydrogen-bonding interaction between Thr95 and the heme-bound O_2 would be responsible for the selective O_2 sensing and the intramolecular signal transduction upon O_2 binding.
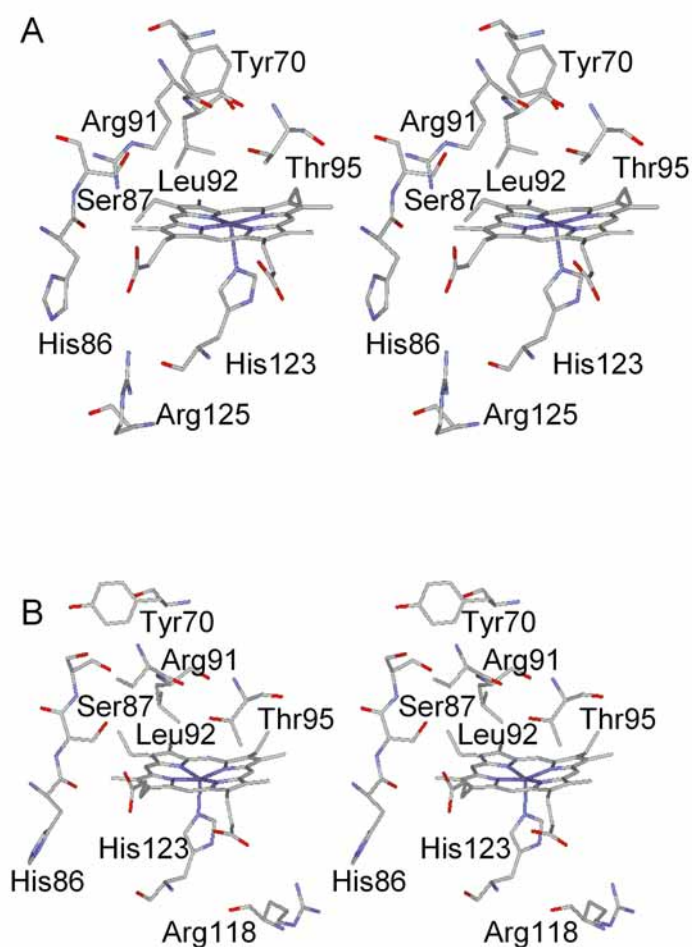

Figure 1.   Stereo views of the heme environmental structures of deoxy HemAT-*Bs* (A) subunit A and (B) subunit B (PDB: 1OR6).[9]   Depicted residues are Tyr70, Leu92, Thr95, His123, and the amino acids with a polar side chain that are located within 5 Å from the heme propionates.

27

In this study, the author characterized the coordination structure of the heme, and the hydrogen-bonding pattern on the heme-bound ligands and on the heme propionates in O_2-, CO-, and NO-bound forms of wild type (WT) and several mutants of full-length HemAT-Bs to investigate the mechanism of the selective O_2 sensing by HemAT-Bs. On the basis of these results, the author shows that the formation of a hydrogen bond between His86 and the heme propionate 6 upon O_2 binding causes a protein conformational change that allows Thr95 to form a specific hydrogen bond to the heme-bound O_2.

Experimental Procedure

Protein expression and purification

In this study, the author used full-length HemAT-Bs with a C-terminal His_6-tag, which was expressed in *E. coli* BL21(DE3) under the control of T7 promoter in pET-24(+) vector (Novagen). Site-directed mutagenesis was carried out using QuikChange Site-directed Mutagenesis Kit (Stratagene). For the expression of HemAT-Bs, the *E. coli* cells were grown aerobically at 37°C for 4 hours in Terrific Broth containing 30 µg/mL kanamycin. The expression was induced by addition of isopropyl-β-D-thiogalactopyranoside to a final concentration of 1 mM, and then the cultivation was continued at 22°C for 18 hours. The cells were harvested by centrifugation at 4,000 × g and were stored at −78°C until use.

The cells were thawed and resuspended in the buffer A (50 mM Tris-HCl buffer (pH 8.0) containing 15 mM glycine and 1 M NaCl), and then were broken by sonication. The resulting suspension was centrifuged at 100,000 × g for 20 minutes, and the supernatant was loaded on a Ni^{2+}-charged HiTrap Chelating column (GE Healthcare). After washing the column with the buffer A, and then with 50 mM Tris-HCl buffer (pH 8.0), the adsorbed proteins were eluted by 50 mM Tris-HCl buffer (pH 8.0) containing 100 mM imidazole. The fractions containing HemAT-Bs were combined and loaded on a HiTrap Q HP column (GE Healthcare). The column was washed with 50 mM Tris-HCl buffer (pH 8.0) containing 100 mM NaCl, and then HemAT-Bs was eluted by increasing the concentration of NaCl in the buffer. The purity and yield of the sample were checked by SDS-PAGE. A typical result is shown in Figure 2.
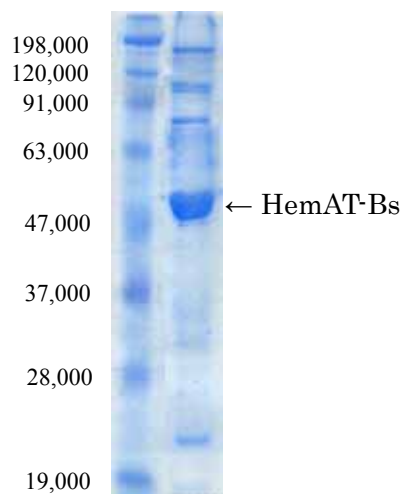
Figure 2. The SDS-PAGE of the purified HemAT-Bs with a Ni^{2+}-charged HiTrap Chelating column and a HiTrap Q HP column.

Sample preparation for measurements

HemAT-Bs was oxidized by adding a small amount of potassium ferricyanide. Excess potassium ferricyanide was removed by using a PD10 column (Amersham Biosciences Corp.) with 50 mM Tris-HCl buffer (pH 8.0). Five times excess amount of sodium dithionite was added into degassed ferric HemAT-Bs solution to make ferrous HemAT-Bs. To prepare CO-, NO-, and O_2-bound HemAT-Bs, the ferrous HemAT-Bs solution was exposed to CO, NO, and O_2 gas, respectively.

Spectroscopic methods

EPR spectra of NO-bound HemAT-Bs were measured at 20 K on a Bruker ESP300E spectrometer with the microwave frequency of 9.5 GHz and the modulation amplitude of 5.0 G.

Resonance Raman spectra of HemAT-Bs were measured as reported previously (12,13). Excitation source were a Kr^+ laser (Spectra Physics 2060) at 413.1 nm and 406.7 nm for the O_2- and

CO-bound forms, and for the NO-bound form, respectively. The scattered light was dispersed with a single polychromator (Ritsu DG-1000) equipped with a liquid nitrogen-cooled charge-coupled device camera. Obtained Raman shifts were calibrated using indene and aqueous solution of potassium ferrocyanide. The laser power was 0.2 mW for the CO-bound form and 1 mW for the O_2- and NO-bound forms at the sample point.

In the resonance Raman spectra of O_2-bound HemAT-Bs, some isotope ($^{16}O_2$ and $^{18}O_2$)-insensitive bands overlap with the Fe—O_2 stretching bands. Gaussian-bands fitting analyses of the resonance Raman spectra of the O_2-bound forms were carried out with Igor Pro 5.03 for distinguishing the Fe—O_2 modes from other isotope-insensitive modes.[12] The width, peak position, and intensity ratio for the isotope-insensitive modes were fixed for the fitting of $^{16}O_2$ and $^{18}O_2$ spectra.

Results

Absorption spectra of the CO- and NO-bound HemAT-Bs

The electronic absorption spectra of the CO-bound form of WT, T95A, and Y70F HemAT-Bs showed the Soret, β and α peaks at 422, 542, and 566 nm, respectively (Figure 3A). These spectra are typical of CO-bound heme proteins with a 6-coordinated, low-spin heme. All of the NO-bound form of WT, T95A, and Y70F HemAT-Bs gave the same spectra with the Soret, β, and α peaks at 419, 548, and 575 nm, respectively (Figure 3B). These spectra are typical of a 6-coordinate, low-spin Fe(II) nitrosyl heme with a proximal histidine ligand, as seen in NO-bound myoglobin (Mb).[14]
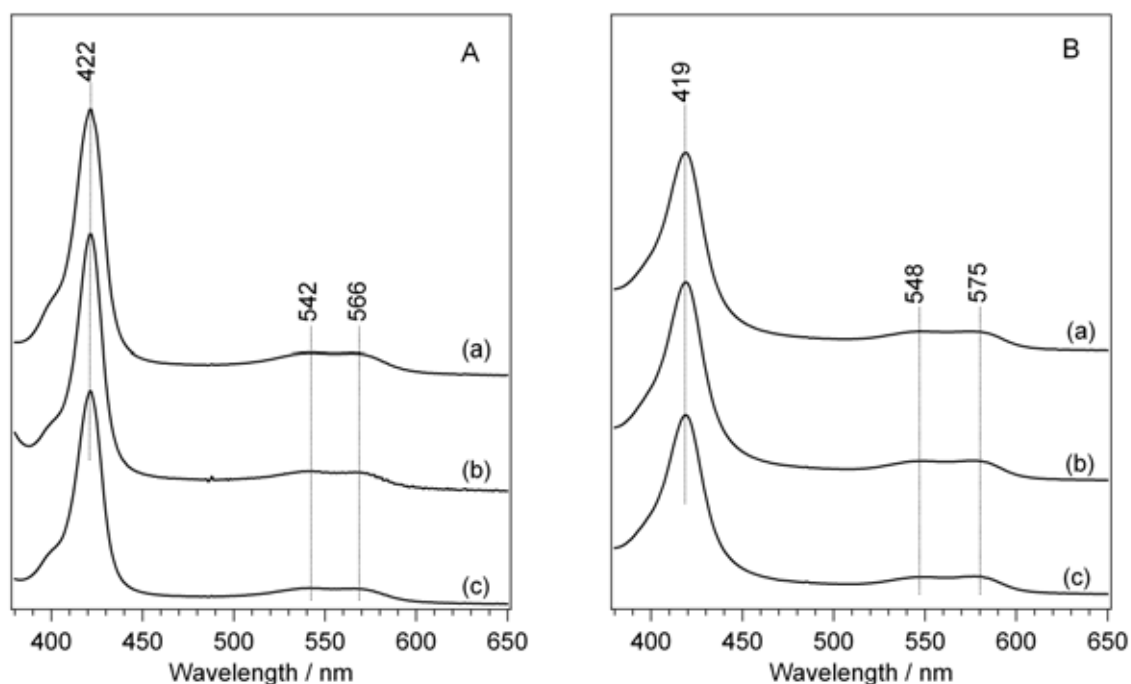

Figure 3. Electronic absorption spectra of (A) CO-bound and (B) NO-bound HemAT-Bs. (a) WT, (b) T95A, and (c) Y70F HemAT-Bs

EPR spectra of the NO-bound HemAT-Bs

Figure 3 shows the EPR spectra of NO-bound HemAT-Bs. The first derivative spectrum with g = 2.08, 2.01, and 1.97 was typical of a 6-coordinated Fe(II) nitrosyl heme (Figure 4A).[15] In the second derivative spectrum, nine hyperfine splitting signals (a triplet of triplets) were observed as the result of the hyperfine interaction with both of ^{14}N nuclei of NO (A_1) and the trans axial His (A_2). The hyperfine coupling constants derived from the nitrogen atoms of the heme-bound NO and the proximal histidine were determined to be A_1 = 2.2 mT and A_2 = 0.6 mT, respectively (Figure 4B). The EPR spectra of T95A and Y70F HemAT-Bs were the same as that of WT (Figure 4C). These results indicate the formation of a 6-coordinated nitrosyl heme with a proximal histidine in the NO-bound form, which is consistent with the results of the electronic absorption spectroscopy.
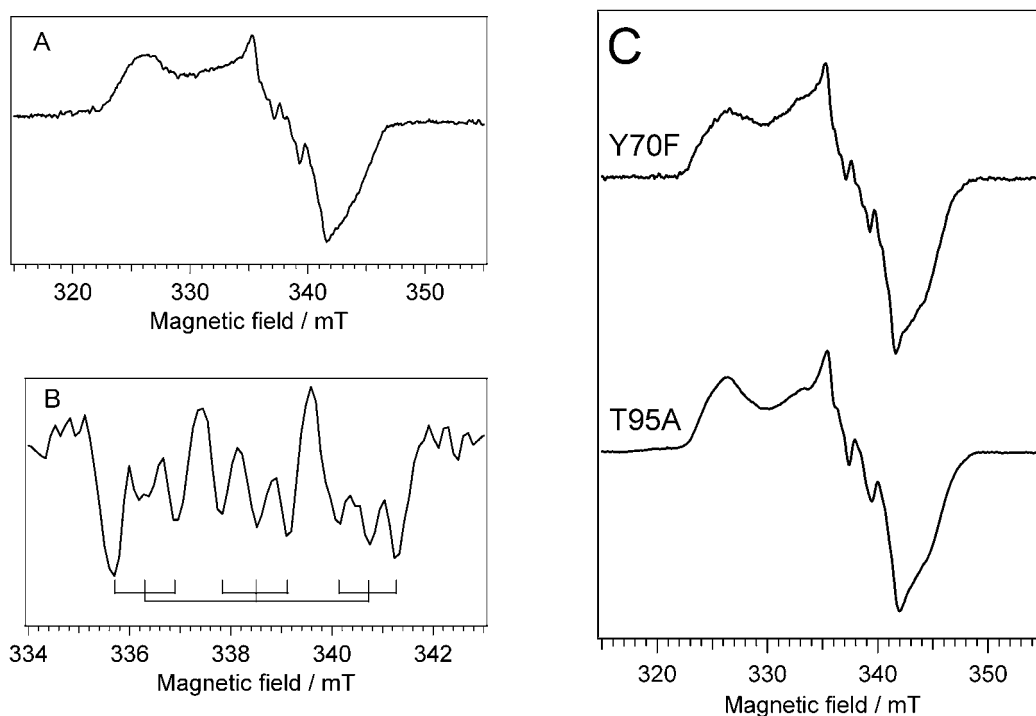

Figure 4. (A) The first derivative EPR spectrum and (B) the second derivative EPR spectrum of NO-bound WT HemAT-*Bs* in 50 mM Tris-HCl buffer (pH 8.0). These spectra were recorded at 20K with microwave frequency of 9.5 GHz, and modulation amplitude of 5.0 G.

Resonance Raman spectroscopy for the CO-bound HemAT-Bs

Fe—C and C—O stretching frequencies of CO-bound heme proteins, $\nu_{Fe—CO}$ and $\nu_{C—O}$, are sensitive and reliable markers for the electrostatic environment around the heme-bound CO.[16] The $\nu_{Fe—CO}$ and $\nu_{C—O}$ bands of CO-bound WT HemAT-Bs were observed at 495 cm^{-1} and 1966 cm^{-1}, respectively (Figure 5). These values were similar to those of H64I ($\nu_{Fe—CO}$ = 490 cm^{-1}, $\nu_{C—O}$ = 1968 cm^{-1}) and H64L ($\nu_{Fe—CO}$ = 490 cm^{-1}, $\nu_{C—O}$ = 1965 cm^{-1}) Mbs,[17] but different from those of WT Mb ($\nu_{Fe—CO}$ = 512 cm^{-1}, $\nu_{C—O}$ = 1944 cm^{-1}).[18] These results indicate that the heme-bound CO is in a hydrophobic environment without any electrostatic interaction in WT HemAT- Bs.

T95A HemAT-Bs gave the similar $\nu_{Fe—CO}$ and $\nu_{C—O}$ values to those of WT HemAT-Bs, indicating that the environment around the CO in T95A HemAT-Bs is also hydrophobic without electrostatic interaction on the CO and that the mutation of Thr95 makes little effect on the environment around the heme-bound CO. On the other hand, Y70F HemAT-Bs showed different resonance Raman spectra from those of WT and T95A HemAT-Bs. Two $\nu_{C—O}$ bands were observed at 1961 and 1945 cm^{-1} in Y70F HemAT-Bs (Figure 5). Furthermore, a weak shoulder around 510 cm^{-1} was observed in the $\nu_{Fe—CO}$ region of Y70F HemAT-Bs, which may correlate with the new $\nu_{Fe—CO}$ band observed at 1945 cm^{-1}. These results suggest the existence of two conformers of Fe-CO unit with different environments around the heme-bound CO in this mutant.

In the crystal structure of the subunit A in the deoxy form of the HemAT-Bs sensor domain,[11] the phenyl oxygen atom of Tyr70 side chain is just above the heme iron atom with the distance of 5.8 Å. This fact implies that the non-bonding electron pair on the oxygen atom of the phenyl group of Tyr70 would interact with the oxygen atom of the heme-bound CO. The 5 cm^{-1} low-frequency shift seen in the $\nu_{C—O}$ band of Y70F HemAT-Bs (the $\nu_{C—O}$ at 1961 cm^{-1}) is consistent with the disappearance of this interaction by the mutation. In addition, the oxygen atom of Tyr70 side chain is close to the carbonyl oxygen atom of Leu92 with the distance of 2.9 Å, which is consistent with the presence of a hydrogen bond between Tyr70 and Leu92.[11] Disappearance of this hydrogen bond in Y70F mutant would cause a considerable conformational perturbation in the distal heme pocket. The new $\nu_{C—O}$ band at 1945 cm^{-1} and a weak shoulder at ca 510 cm^{-1} seen in this mutant might be caused by this structural perturbation.

Zhang *et al.* reported that Tyr70 mutants of the HemAT-Bs sensor domain showed the large dissociation constants for the heme-bound O_2, and proposed that Tyr70 would form a hydrogen bond to the heme-bound O_2 on the basis of these results.[6] Our previous results, however, have shown that Tyr70 does not form such a hydrogen bond in the full-length of HemAT-Bs.[12] Their results will imply that Tyr70 is responsible for the fixation of the position of Thr95 that forms the hydrogen bond with the heme-bound O_2. Leu92 and Thr95 are located in the same helix, the E-helix. If the hydrogen bond between Leu92 and Tyr70 disappear, the position of the E-helix would be perturbed, resulting in low stability of the O_2-bound form of Tyr70 mutants. In addition, the author have also shown that hydrogen-bonding pattern around the heme-bound O_2 is different between the full-length and the truncated sensor domain of HemAT-Bs.[12] These results suggest that the affinity of O_2 and the hydrogen-bonding interaction around the heme-bound O_2 are different between the truncated sensor domain and the full-length of HemAT-Bs.
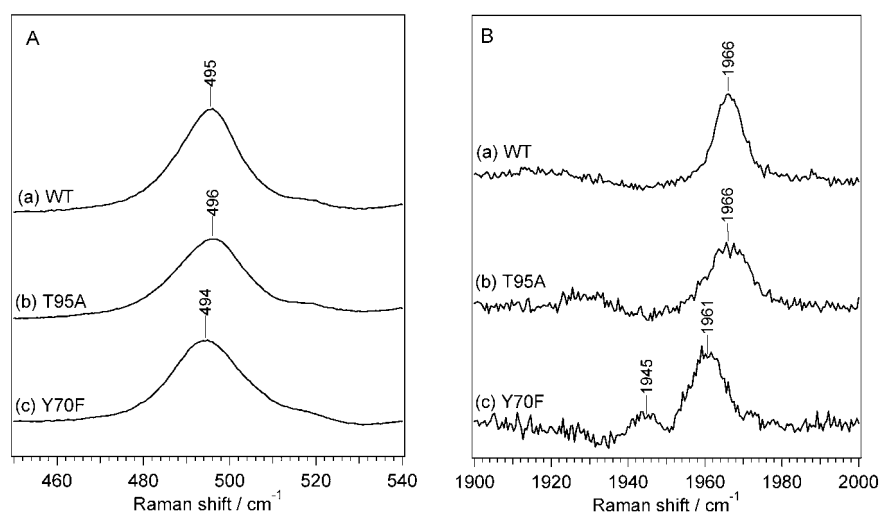

Figure 5.　Resonance Raman spectra of CO-bound (a) WT, (b) T95A, and (c) Y70F HemAT-*Bs*.　(A) Fe—CO stretching bands in the low frequency region.　(B) C-O stretching bands in the high frequency region.

Table 1. The frequencies of the Fe—CO and C—O stretching band

Proteins	ν_{Fe-CO} / cm^{-1}	ν_{C-O} / cm^{-1}	Ref.
HemAT WT	495	1966	this work
HemAT T95A	496	1966	this work
HemAT Y70F	494	1945, 1961	this work
swMb WT	512	1944	18
swMb H64I	490	1968	17
swMb H64L	490	1965	17

Resonance Raman spectroscopy for the NO-bound HemAT-Bs

The high frequency region in the resonance Raman spectra of heme proteins contain some marker bands sensitive to the oxidation state (ν_4), and the spin and coordination state (ν_2 and ν_3) of the heme iron. In the case of NO-bound HemAT-Bs, the ν_4, ν_3, and ν_2 band were observed at 1373, 1498, and 1577 cm^{-1}, respectively (Figure 6). These results are typical of the 6-coordinated low-spin heme, and consist with the results from UV-Vis and EPR spectroscopies.
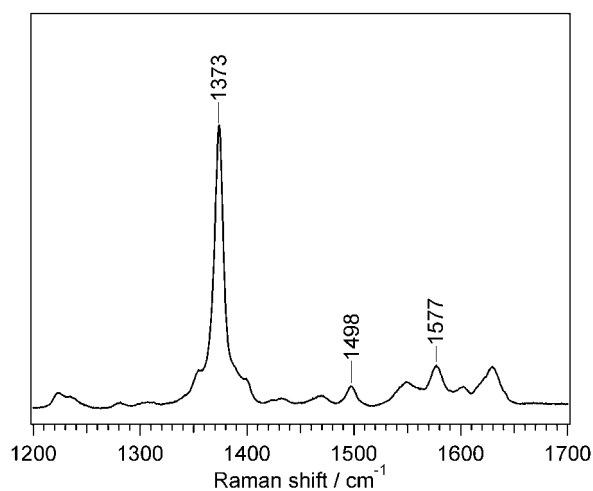

Figure 6. The resonance Raman spectrum of NO-bound HemAT WT in the high frequency region.

N—O stretching frequency, $\nu_{N—O}$, of NO-bound heme proteins is also affected by the heme distal environments.[19] The $\nu_{N—O}$ band of WT HemAT-Bs was observed at 1636 cm^{-1} (Figure 7). This value was similar to that of the $\nu_{N—O}$ of H64L Mb ($\nu_{N—O}$ = 1635 cm^{-1}), but not to that of WT Mb ($\nu_{N—O}$ = 1613 cm^{-1}).[19] These results suggest that the heme-bound NO in WT HemAT-Bs is in a hydrophobic environment without any electrostatic interaction with the heme-bound NO.

The Fe—NO stretching mode, $\nu_{Fe—NO}$, of NO-bound WT HemAT-Bs was observed at 545 cm^{-1} (Figure 7). The $\nu_{Fe—NO}$ band is not sensitive to the electrostatic environment of the distal heme pocket.[19] Rather, the $\nu_{Fe—NO}$ frequency is reported to be dependent on the Fe-N-O angle.[20] This

frequency is lowered by decreasing of the Fe-N-O angle.[20]   The ν_{Fe-NO} frequency of NO-bound HemAT-Bs (545 cm^{-1}) was lower than that of NO-bound Mb (558 cm^{-1}),[19] suggesting that Fe-N-O angle in NO-bound HemAT-Bs is lower than that in NO-bound Mb.
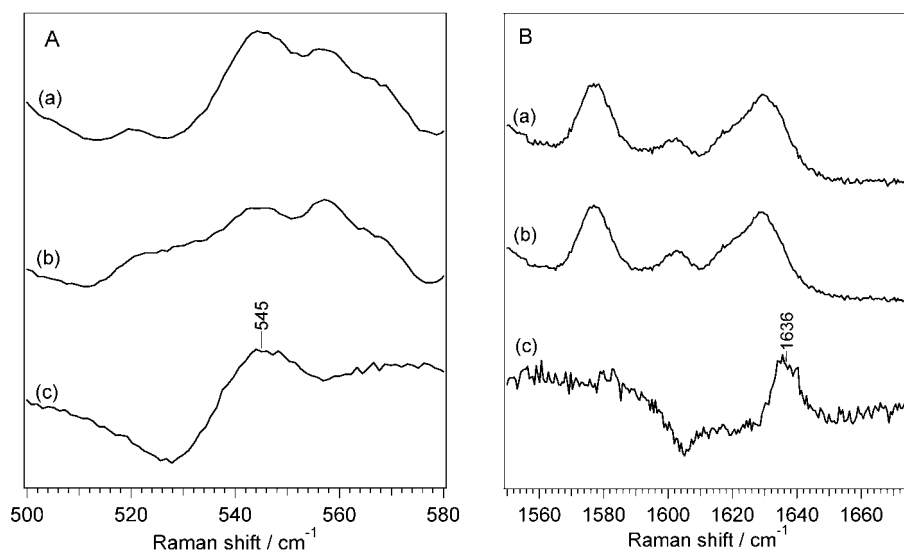

Figure 7.   Resonance Raman spectra of NO-bound HemAT-*Bs*.   (a) [14]NO-bound WT HemAT-*Bs*, (b) [15]NO-bound WT HemAT-*Bs*, (c) (a)-(b) difference spectrum.

Table 2. The frequencies of the Fe—NO and N—O stretching band

Proteins	ν_{Fe-NO} / cm^{-1}	ν_{N-O} / cm^{-1}	Ref.
HemAT WT	545	1636	this work
HemAT T95A	545	1635	this work
HemAT Y70F	556	1637	this work
swMb WT	560	1613	19
swMb H64L	560	1635	19
swMb H64G	560	1631	19

38

The heme propionate bending mode, $\delta(C_\beta C_c C_d)$, in the resonance Raman spectra of HemAT-Bs

The bending mode of the heme propionate, $\delta(C_\beta C_c C_d)$, in the resonance Raman spectra of O_2-bound HemAT-Bs showed a different feature from those of the ferrous, CO-, and NO-bound forms. The resonance Raman spectra of ferrous, CO-, and NO-bound HemAT-Bs showed one $\delta(C_\beta C_c C_d)$ band at 365, 373, and 375 cm^{-1}, respectively (Figure 8). On the other hand, in the O_2-bound form, two $\delta(C_\beta C_c C_d)$ bands were observed at 370 and 383 cm^{-1}, suggesting that there are two species with different conformations around the heme propionates in O_2-bound HemAT-Bs.

The $\delta(C_\beta C_c C_d)$ band is sensitive to electrostatic interaction on the heme propionate(s), *e.g.* hydrogen bonds and salt bridges.[21] The stronger electrostatic interaction between the heme propionate(s) and surrounding residue(s), the higher frequency of the $\delta(C_\beta C_c C_d)$ band.[21] The $\delta(C_\beta C_c C_d)$ band at 365, 373, 375, and 370 cm^{-1} in ferrous, CO-, NO-, and O_2-bound HemAT-Bs, respectively, are lower than those of the corresponding forms of Mb (371, 377, 378, and 378 cm^{-1} for the ferrous, CO-, NO-, and O_2-bound forms, respectively) in which moderate hydrogen bonds exist on the heme propionate 7.[19,22-24] These results indicate that the conformers showing these $\delta(C_\beta C_c C_d)$ bands have no or a weak hydrogen bond on the heme propionate.

The additional $\delta(C_\beta C_c C_d)$ band at 383 cm^{-1} in O_2-bound HemAT-Bs indicates the existence of a stronger hydrogen bond or a salt bridge on the heme propionate. This conformer was observed only in the O_2-bound form. To determine the amino acid residue(s) responsible for the 383 cm^{-1} band, the author prepared the following five mutants: H86A, S87A, R91A, R118A, and R125A, in which every polar residue within 5 Å from the heme propionates is mutated to alanine (Figure 1). The $\delta(C_\beta C_c C_d)$ band at 383 cm^{-1} disappeared only in O_2-bound H86A HemAT-Bs, while other mutants (S87A, R91A, R118A and R125A HemAT-Bs) showed almost the same $\delta(C_\beta C_c C_d)$ band at 383 cm^{-1} as that of WT HemAT-Bs (Figure 9). The 370 cm^{-1} band seen in the spectrum of WT exhibited 5 cm^{-1} upshift by the mutation of His86 and Ser87, both of which are located in the CE-loop near the heme propionate. This upshift of the 370 cm^{-1} band might be caused by a structural perturbation around the heme propionate. These results indicate that His86 is the residue that forms the hydrogen bond with the one of the heme propionate, probably the one at the position 6,

and that the residues in the CE-loop are responsible to maintain the proper structure around the heme propionate.
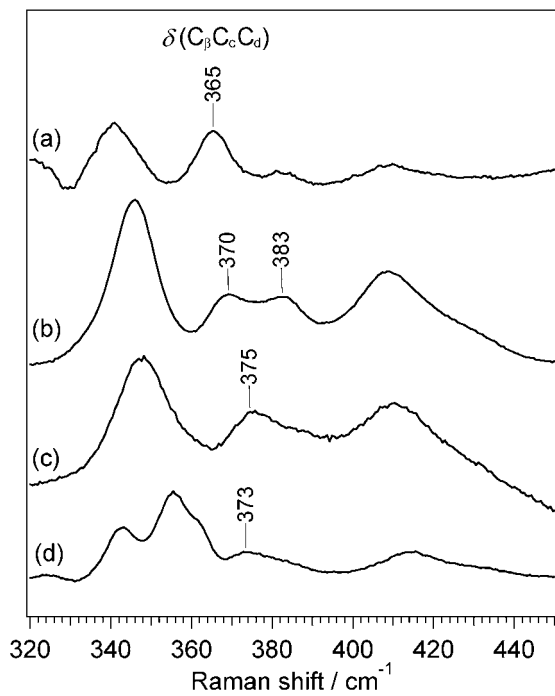

Figure 8. Resonance Raman spectra of WT HemAT-*Bs* in the (a) ferrous, (b) O$_2$-bound, (c) NO-bound, and (d) CO-bound forms.
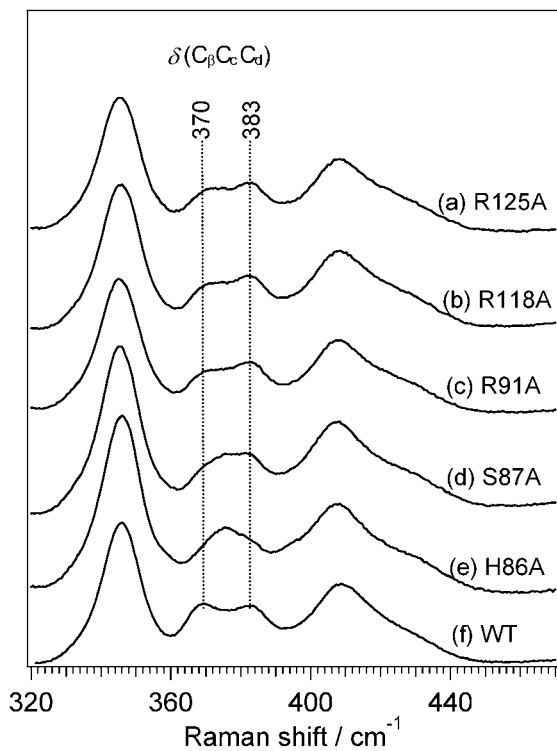

Figure 9. Resonance Raman spectra of O$_2$-bound form of (a) R125A, (b) R118A, (c) R91A, (d) S87A, (e) H86A, and (f) WT HemAT-*Bs*.

The hydrogen bonding pattern to the heme-bound O$_2$ in the O$_2$ bound form of H86A HemAT-Bs

The Fe—O$_2$ stretching frequency region of the resonance Raman spectrum of H86A HemAT-Bs was also different from that of WT HemAT-Bs. Three $\nu_{Fe—O2}$ bands were observed at 554, 566, and 572 cm^{-1} in O$_2$-bound WT HemAT-Bs, as shown in the Introduction. In H86A HemAT-Bs, the band at 566 cm^{-1} disappeared, and only the bands at 557 and 572 cm^{-1} were observed as shown in Figure 10. These bands were shifted to 538 and 554 cm^{-1}, respectively, upon $^{18}O_2$ substitution. These isotope shifts of 19 and 18 cm^{-1} were consistent with the previously reported values for WT HemAT-Bs and in agreement with a calculated shift value of 21 cm^{-1}.[12] The $^{16}O_2$ - $^{18}O_2$ difference spectrum was also consistent with the result of the Gaussian fitting analysis (Figure 10(C)). The difference in the Fe—O—O bond angle affects the shift of the Fe—O$_2$ stretching mode upon the isotope substitution of O$_2$, which will cause a slight difference between the experimental and calculated values of the isotope shift. These results indicate that the loss of the hydrogen bond between His86 and the heme propionate 6 affects the hydrogen-bonding interaction between the heme-bound O$_2$ and Thr95.
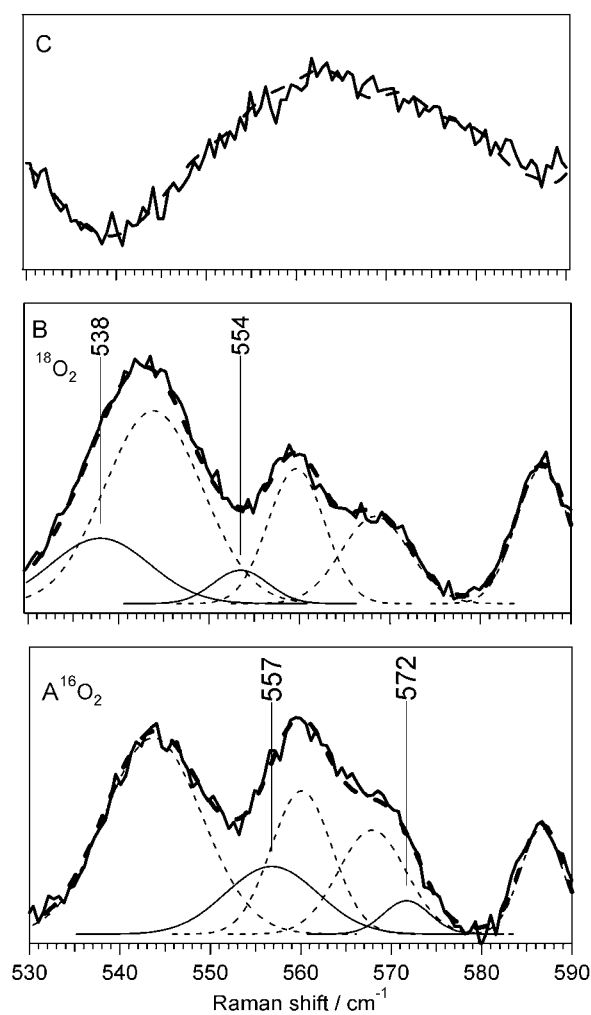
Figure 10. Resonance Raman spectra of (A) $^{16}O_2$-bound H86A HemAT-*Bs*, (B) $^{18}O_2$-bound H86A HemAT-*Bs*. The bold solid lines are the raw spectra. All traces except for the bold solid lines were obtained by Gaussian band fitting analysis. The thin solid lines denote contribution from ν_{Fe-O2}, which were sensitive to the isotope substitution of O_2. The thin dotted lines are due to the isotope-insensitive modes. The bold dotted lines are the sum of the component bands. (C) The $^{16}O_2 - ^{18}O_2$ difference spectra. The broken line in the spectrum (C) is the difference spectrum obtained the Gaussian band fitting analysis. The bold solid line is the experimental difference spectrum.

Discussion

It is a critical requirement for the heme-based gas sensor proteins to discriminate between the effector gas molecule and other gas molecules. Some heme-based gas sensor proteins, such as CooA and sGC, alter the coordination number (5-coordinate vs. 6-coordinate) of the heme depending on the species of heme-bound gas molecules.[25-27] The proper coordination structure with the effector molecule causes a protein conformational change that is essential to a specific response to the cognate effectors. The heme of HemAT-Bs, however, has a 6-coordinate structure in all of the O_2-, CO-, and NO-bound forms, indicating that HemAT-Bs does not adopt this strategy for the selective O_2 sensing.

Another possible strategy for the heme-based gas sensor proteins to discriminate the effector gas molecule is to form a specific interaction between the heme-bound effector molecule and neighboring amino acid residues. The author have reported that Thr95 forms the hydrogen bonds to the heme-bound O_2 in the two conformers among the three ones in the O_2-bound form.[12] On the other hand, the author has revealed here that no hydrogen bond is formed on the heme-bound ligand in the case of CO- and NO-bound HemAT-Bs. These results show that the hydrogen bonding between a heme-bound ligand and Thr95 is specific in the O_2-bound form, which supports the idea that this hydrogen bonding interaction is essential for the selective O_2 sensing by HemAT-Bs.

The crystal structure of the HemAT-Bs sensor domain in the ferrous form shows that the distances between the hydroxyl oxygen atom of Thr95 and the heme iron atom are 6.8 and 7.6 Å in the subunits A and B, respectively.[11] To form the direct hydrogen bond to the heme-bound O_2, Thr95 has to be located within 3 Å from the heme iron. Although the above distances in the ferrous form are too long to form a hydrogen bond, a direct hydrogen bond is certainly formed between Thr95 and the "proximal" oxygen atom of the heme-bound O_2.[12] These results indicate that the formation of the hydrogen bond between Thr95 and the proximal oxygen atom requires a preceding conformational change of the distal heme pocket that moves Thr95 to the suitable position to form the hydrogen bond.

Because the O_2-bound H86A HemAT-Bs cannot form the conformer with the direct hydrogen bond between Thr95 and the proximal oxygen atom, the preceding conformational alteration would be induced by the formation of the hydrogen bond between His86 and the heme propionate 6, as discussed below.   His86 is located in the CE-loop, which is adjacent to the E-helix that contains Thr95.   The formation of the hydrogen bond between His86 and the heme propionate 6, which takes place only upon O_2 binding, will induce a conformational change of the CE-loop.   And then, this conformational alteration of the CE-loop will propagate to the E-helix, finally shifting Thr95 to the proper position to form the direct hydrogen bond to the proximal oxygen atom.   Thus, HemAT-Bs would cause a stepwise conformational change upon O_2 binding.

If Thr95 were located in advance at the suitable position to form the hydrogen bond to the heme-bound O_2 in ferrous form, Thr95 would also form a similar hydrogen bond to the heme-bound CO and NO.   In this situation, the hydrogen bond between Thr95 and the heme-bound O_2 could not be used for the selective O_2 sensing.   The stepwise conformational change upon O_2 binding allows the hydrogen bond between Thr95 and the heme-bound ligand to be specific for the O_2-bound form.

On the basis of these results, the author proposes the heme environmental structure of O_2-bound HemAT-Bs as shown in Figure 11.   Three conformers exist in O_2-bound HemAT-Bs with different hydrogen bonding interactions on the heme-bound O_2, corresponding to the closed, the open α, and the open β forms.[12]   Hydrogen bonding interaction on the heme propionate is also different among these three conformers.   His86 forms the hydrogen bond to the heme propionate in the open α form in which the direct hydrogen bond is formed between Thr95 and the heme-bound O_2.   His86 does not form the hydrogen bond with the heme propionate in the closed and the open β forms in which Thr95 does not come close to the heme-bound O_2.

Figure 11. The conformations around the heme in the O_2-bound form of HemAT-Bs

HemAT-Bs should undergo a sufficient conformational change upon O_2 binding for generating the aerotactic signal. The formation of the open α form involves a considerable conformational change of the CE-loop and the E-helix, suggesting that the open α form is the "on-state" for the signaling. In the closed and open β forms, the conformational change of the CE-loop and the E-helix will not be so large because the hydrogen bond is not formed between His86 and the heme propionate. Therefore, the closed and the open β forms will be the "off-state". It remains to be elucidated why the on- and off-states exist together in O_2-bound HemAT-Bs, and whether the closed and open β forms have any physiological role.

In summary, the author proposes the following mechanism for the selective O_2 sensing and the signal transduction in HemAT-Bs. When O_2 is bound to the heme in HemAT-Bs, the hydrogen bond forms between His86 and the heme propionate 6. The formation of this hydrogen bond makes a conformational alteration in the distal heme pocket, especially on the position of the E-helix. The change in the position of the E-helix makes Thr95 to be located at the suitable position to form the hydrogen bond with the proximal oxygen atom of the heme-bound O_2. As the hydrogen bond is not formed between His86 and the heme propionate 6 upon CO and NO binding, the proper conformational change does not occur in these cases. The proper conformational change around the heme upon O_2 binding will propagate to the signaling domain of HemAT-Bs, and then activate CheA.

REFERENCES

1. Rodgers, K.R. (1999) Heme-based sensors in biological systems, *Curr. Opin. Chem. Biol. 3*, 158-167

2. Chan, M. K. (2001) Recent advances in heme-protein sensors, *Curr. Opin. Chem. Biol. 5*, 216-222

3. Jain, R., and Chan, M. K. (2003) Mechanisms of ligand discrimination by heme proteins, *J Biol. Inorg. Chem. 8*, 1-11

4. Hou, S., Larsen, R. W., Boudko, F., Riley, C. W., Karatan, E., Zimmer, M., Ordal, G. W. and Alam, M. (2000) Myoglobin-like aerotaxis transducers in Archaea and Bacteria, *Nature 403*, 540-544

5. Aono, S., Kato, T., Matsuki, M., Nakajima, H., Ohta, T., Uchida, T., and Kitagawa, T., (2002) Resonance Raman and ligand binding studies of the oxygen-sensing signal transducer protein HemAT from *Bacillus subtilis*, *J. Biol. Chem. 277,* 13528-13538

6. Zhang, W., Olson, J. S. and Phillips, G. N. Jr. (2005) Biophysical and kinetic characterization of HemAT, an aerotaxis receptor from *Bacillus subtilis, Biophys. J. 88*, 2801-2814

7. Ohta, T. and Kitagawa, T. (2005) Resonance Raman investigation of the specific sensing mechanism of a target molecule by gas sensory proteins, *Inorg. Chem. 44*, 758-769

8. Szurmant, H. and Ordal, G. W. (2004) Diversity in chemotaxis mechanisms among the bacteria and archaea, *Microbiol. Mol. Biol. Rev. 68*, 301-319

9. Bischoff, D. S. and Ordal, G. W (1992) *Bacillus subtilis* chemotaxis: a deviation from the *Escherichia coli* paradigm, *Mol. Microbiol. 6*, 23-28

10. Garrity, L. F. and Ordal G, W. (1995) Chemotaxis in *Bacillus subtilis*: how bacteria monitor environmental signals, *Pharmac. Ther. 68*, 87-104

11. Zhang, W. and Phillips, G. N. Jr. (2003) Structure of the oxygen sensor in *Bacillus subtilis*: signal

transduction of chemotaxis by control of symmetry, *Structure 11*, 1097-1110

12. Ohta, T., Yoshimura, H., Yoshioka, S., Aono, S. and Kitagawa, T. (2004) Oxygen-sensing mechanism of HemAT from *Bacillus subtilis*: A resonance Raman spectroscopic study, *J. Am. Chem. Soc. 126*, 15000-15001

13. Aono, S., Nakajima, H., Ohta, T. and Kitagawa, T. (2004) Resonance Raman and ligand-binding analysis of the oxygen-sensing signal transducer protein HemAT from *Bacillus subtilis*, *Methods Enzymol. 381*, 618-628

14. Yoshimura, T. and Ozaki, T. (1984) Electronic-spectra for nitrosyl(protoporphyrin-IX dimethyl ester)iron(II) and its complexes with nitrogenous bases as model systems for nitrosylhemoproteins, *Arch. Biochem. Biophys. 229*, 126-135

15. Yoshimura, T., Ozaki, T., Shintani, Y. and Watanabe, H. (1979) Electron-paramagnetic resonance of nitrosylprotoheme dimethyl ester complexes with imidazole derivatives as model systems for nitrosylhemoproteins, *Arch. Biochem. Biophys. 193*, 301-313

16. Spiro, T.G., Wasbotten, I. H. (2005) CO as a vibrational probe of heme protein active site, *J. Inorg. Biochem.*, *99*, 34-44

17. Li, T. S., Quillin, M. L., Phillips G. N. Jr. and Olson, J. S. (1994) Structural determinants of the stretching frequency of CO bound to myoglobin, *Biochemistry 33*, 1433-1446

18. Tsubaki, M., Srivastava, R. B. and Yu, N. T. (1982) Resonance Raman investigation of carbon monoxide bonding in (carbon monoxy) hemoglobin and -myoglobin: detection of iron-carbon monoxide stretching and iron-carbon-oxygen bending vibrations and influence of the quaternary structure change, *Biochemistry 21*, 1132-1140

19. Tomita, T., Hirota, S., Ogura, T., Olson, J. S. and Kitagawa, T. (1999) Resonance Raman investigation of Fe-N-O structure of nitrosylheme in myoglobin and its mutants, *J. Phys. Chem. B 103*, 7044-7054

20. Hu, S. and Kincaid, J. R. (1991) Resonance Raman characterization of nitric oxide adducts of cytochrome P450cam: the effect of substrate structure on the iron-ligand vibrations, *J. Am. Chem.*

Soc. 113, 2843-2850

21.   Uchida, T. and Kitagawa, T. (2005) Mechanism for transduction of the ligand-binding signal in heme-based gas sensory proteins revealed by resonance Raman spectroscopy, *Acc. Chem. Res. 38* 662-670

22.   Peterson, E. S., Friedman, J. M., Chien, E. Y. T. and Sligar, S. G. (1998) Functional implications of the proximal hydrogen-bonding network in myoglobin: a resonance Raman and kinetic study of Leu89, Ser92, His97, and F-helix swap mutants, *Biochemistry 37*, 12301-12319

23.   Hirota, S., Ogura, T., Shinzawa-Itoh, K., Yoshikawa, S., Nagai, M. and Kitagawa, T. (1994) Vibrational assignments of the FeCO unit of CO-bound heme proteins revisited: Observation of a new CO-isotope-sensitive Raman band assignable to the FeCO bending fundamental, *J. Phys. Chem. 98*, 6652-6660

24.   Hirota, S., Ogura, T., Appelman, E. H., Shinzawa-Itoh, K., Yoshikawa, S. and Kitagawa, T. (1994) Observation of a new oxygen-isotope sensitive Raman band for oxyhemoproteins and its implications in heme pocket structures, *J. Am. Chem. Soc. 116*, 10564-10570

25.   Traylor, T. G. and Sharma, V. S. (1992) Why NO?, *Biochemistry 31*, 2847-2849

26.   Russwurm, M. and Koesling, D. (2004) NO activation of guanylyl cyclase, *EMBO J. 23*, 4443-4450

27.   Aono, S (2003) Biochemical and biophysical properties of the CO-sensing transcriptional activator CooA, *Acc. Chem. Res. 36*, 825-831

Chapter 3: Signal transduction through the proximal heme pocket in HemAT-Bs upon ligand binding revealed by time-resolved resonance Raman spectroscopy

Biochemistry. submitted

Abstract

In this chapter, the author investigated on the signal transduction pathway in HemAT-Bs through the proximal heme pocket. According to the crystal structures of HemAT-Bs sensor domain, the distance between the proximal His, His123, and Tyr133 decreases upon CN binding, suggesting the formation of a hydrogen bonding between these residues upon ligand binding. To confirm this, the author measured the time-resolved resonance Raman spectra of full-length HemAT-Bs WT and Y133F in the deoxy form and the photoproduct after photolysis of CO-bound form. In WT, the $\nu_{Fe—His}$ band for the 10 ps photoproduct was observed at higher frequency by about 2 cm^{-1} compared with that of the deoxy form. This difference is relaxed in hundreds of picoseconds. This frequency differences in WT HemAT-Bs would reflect the conformational alteration of the protein matrix. On the other hand, Y133F mutant does not show a substantial $\nu_{Fe—His}$ frequency shift after photolysis. Since hydrogen bond to the proximal His induces up shift of the $\nu_{Fe—His}$ frequency, the results in this study indicate that Tyr133 forms a hydrogen bond to the proximal His residue. HemAT-Bs delineate a new mechanism by which the signal transduction is triggered by the formation of a hydrogen bond to the proximal ligand in the proximal heme pocket upon ligand binding.

Introduction

HemAT from *Bacillus subtilis* (HemAT-Bs) is a heme-based O_2 sensor protein functioning in the chemotactic signal transduction system of this bacterium.[1-8] HemAT-Bs consists of two domains: a sensor domain and a signaling domain. The sensor domain has a globin fold with a heme that functions as an O_2-binding site. O_2-binding to the heme induces a protein conformational change that stimulates the downstream of the chemotactic signaling system in *B. subtilis*. An important issue to understand the signal transduction mechanism of HemAT-Bs is to reveal the pathway to transmit the conformational change from the heme to the protein matrix upon O_2 binding. The pathway of the intramolecular signal transduction in HemAT-Bs, however, has only been partially resolved.

The first step of signal transduction in heme-based gas sensor proteins is transmission of the conformational change from the heme-ligand complex to the protein matrix. In general, a heme-based gas sensor proteins have three potential pathways to transmit the conformational change from the heme to the protein matrix: the distal pathway, the heme-peripheral group pathway, and the proximal pathway.[9] The author has investigated about the former two pathways in HemAT-Bs, as described in the Chapter 2. In brief, upon the binding of O_2 to the heme in HemAT-Bs, His86 forms a hydrogen bond to the heme-propionate, accompanied by another hydrogen bond formation between Thr95 and the heme-bound O_2. The formation of these hydrogen bonds would cause a considerable conformational alteration of the protein matrix through the heme peripheral and the distal pathways, respectively. In addition to these signaling pathways, the proximal pathway can also exist and function with these pathways. However, the proximal pathway in HemAT-Bs has not been investigated to date.

According to the reported crystal structure of HemAT-Bs sensor domain,[3] the structural alteration upon ligand binding to the heme is suggested in the proximal heme pocket. In the heme proximal pocket of the CN-binding form, Tyr133 is positioned within the distance possible to form a hydrogen bond to His123, the proximal histidine. Tyr133 in the crystal structure of the deoxy HemAT-Bs sensor domain is further from His123 than the case in the CN-bound form. These facts imply a hydrogen bonding between Tyr133 and His123 upon ligand binding to the heme (Figure 1).

If this is the case, this hydrogen bond formation may be a trigger of a conformational change for the signal transduction.

To test this hypothesis, the author measured the time-resolved resonance Raman (TR3) spectra of the deoxy form and the ligand-photodissociation products of full-length wild-type HemAT-Bs (WT), full-length HemAT-Bs Y133F mutant (Y133F), and the sensor domain of WT HemAT-Bs. The Fe—His stretching band, $\nu_{Fe—His}$, in these spectra is a sensitive marker to the orientation and electrostatic feature of the imidazole of the proximal histidine. The $\nu_{Fe—His}$ band, however, is observed only in the 5-coordinated ferrous form. Therefore, the author compared the resonance Raman spectra of the deoxy HemAT-Bs and the ligand-photodissociated HemAT-Bs. The intermediate immediately after photolysis is thought to retain the structural feature of the protein matrix in the ligand-bound form even with a 5-cooordinated heme. Because photodissociation efficiency of heme-bound O_2 is too low to perform this measurement, we used carbon monoxide (CO) as the ligand. The photodissociation efficiency of heme-bound CO is enough for TR3 measurement. The structural alteration of the heme proximal pocket upon CO binding would be informative to consider about that upon O_2 binding. Because a conformational change in the proximal heme pocket is not induced by direct interaction between the heme-bound ligand and the proximal heme pocket, a conformational change in the heme proximal pocket induced by CO binding would be similar to that induced by O_2 binding. From these spectroscopic measurements, the author estimates the differences of the heme-proximal structure between the deoxy and the ligand-bound form, and between WT and Y133F. The author then discusses about the possibility of the heme-proximal pathway to function as a pathway of the intramolecular signal transduction in HemAT-Bs.
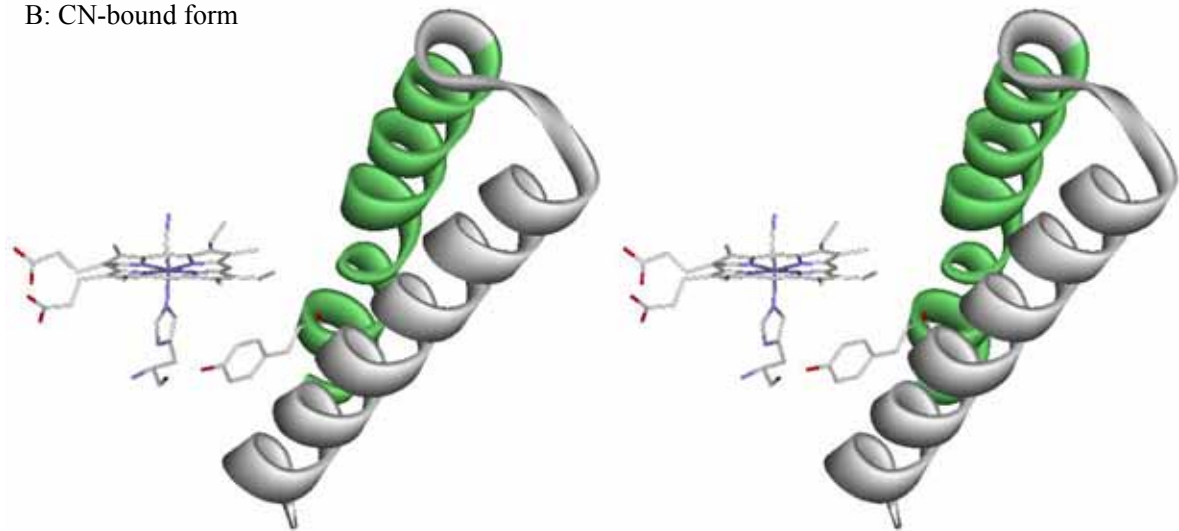
A: deoxy form
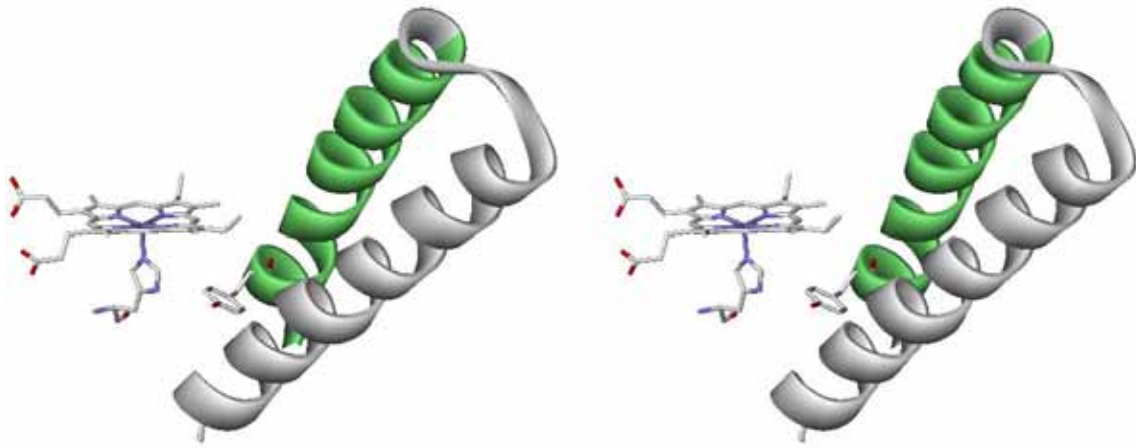
B: CN-bound form

Figure 1. The heme proximal structure and the position of the G and H helices in the deoxy and CN-bound forms in the reported crystal structure of HemAT-Bs sensor domain. The α helix colored in green is the G helix, and white is the H helix. The heme with His123 and the side chain of Tyr133 are shown in stick model.

Experimental Procedure

Protein expression and purification

Full-length and the sensor domain of HemAT-Bs with a C-terminal His_6-tag is expressed and purified with previously described method.[2,7] In brief, *E. coli* BL21(DE3) containing the expression vector of HemAT-Bs was cultivated in Terrific Broth containing 30 μg/mL kanamycin at 37°C for 4h, followed by addition of isopropyl-β-D-thiogalactopyranoside (IPTG) to a final concentration of 1 mM. After the addition of IPTG, the cultivation was continued at 22°C for 18h. The harvested cells suspended in 50 mM Tris-HCl buffer (pH 8.0) were sonicated and then centrifuged. The supernatant containing HemAT-Bs was loaded onto a HisTrap FF column (GE Healthcare), which was then washed with 50 mM Tris-HCl buffer (pH 8.0) containing 15 mM glycine and 500 mM NaCl followed by washing with 50 mM Tris-HCl buffer (pH 8.0). The adsorbed proteins were eluted with 50 mM Tris-HCl buffer (pH 8.0) containing 100 mM imidazole. The eluted fractions containing HemAT-Bs were combined and then loaded onto a HiTrap Q column (GE Healthcare). The adsorbed HemAT-Bs was eluted from the column by increasing NaCl concentration in 50 mM Tris-HCl buffer (pH 8.0).

The expression vector of Y133F was prepared with QuikChange site-directed mutagenesis kit (Stratagene). Two primers (sense primer: 5'-CTTTTGCCAAAATGGTTCATGGGTGCGTTTCAAG-3', anti-sense primer: 5'-CTTGAAACGCACCCATGAACCATTTTGGCAAAAG-3') were used to construct on expression vector of Y133F mutant with the expression vector of wild-type HemAT-Bs as the template. The expression and purification of Y133F was performed with the same method for WT.

The deoxy HemAT-Bs for the TR3 measurement was prepared by addition of excess amount of sodium dithionite to degassed ferric HemAT-Bs solution. The CO-bound form of HemAT-Bs was prepared by exposure of CO gas to the deoxy HemAT-Bs.

Time-resolved resonance Raman spectra measurement

The TR3 spectra in picosecond time resolution were measured as described previously.[10-12] In brief, the probe beam at 442 nm was generated as the first Stokes line in stimulated Raman scattering from methane gas, and the pump beam at 559 nm was generated with an optical parametric generator and amplifier. Both of the beams were produced from the second harmonic of the 784 nm output of a Ti-sapphire laser operated at 1 kHz. The scattered light was detected with a liquid nitrogen-cooled charge-coupled device camera that is attached to a single spectrograph (SPEX, model 500M).

Results

The time-resolved resonance Raman spectra in the low-frequency region

The spectra after photolysis of CO-bound HemAT-Bs were similar to that of the deoxy form (Figure 2). In the spectrum for the deoxy form of WT, the peaks at 300, 340, 364, 408, and 672 cm^{-1} are assigned to the γ_7, ν_8, $\delta(C_\beta C_c C_d)$, $\delta(C_\beta C_a C_b)$, and ν_7 mode of the porphyrin ring, respectively.[13] These bands were observed at almost the same positions in the TR3 spectra for the photoproducts produced by the CO-photodissociation, indicating that the structural relaxation of the porphyrin ring is completed within 10 ps after CO-photodissociation.

The TR3 spectra for the sensor domain of WT showed these bands at substantially the same positions as those of full-length WT. These results indicate that the conformation of the heme in WT is basically the same regardless of the presence or absence of the signaling domain.

These bands in Y133F were observed at almost the same frequencies as those of WT, except for the γ_7 band. The γ_7 band of Y133F was observed at 310 cm^{-1} in the TR3 spectrum for 10 ps photoproduct, and at 312 cm^{-1} in the spectrum for the deoxy form, which are observed at higher frequency by 10 and 12 cm^{-1} than those of WT. The γ_7 mode is a sensitive marker to disorder in the heme pocket.[14] These results, therefore, suggest that Tyr133 would play some roles to maintain the heme proximal pocket with precise conformation.
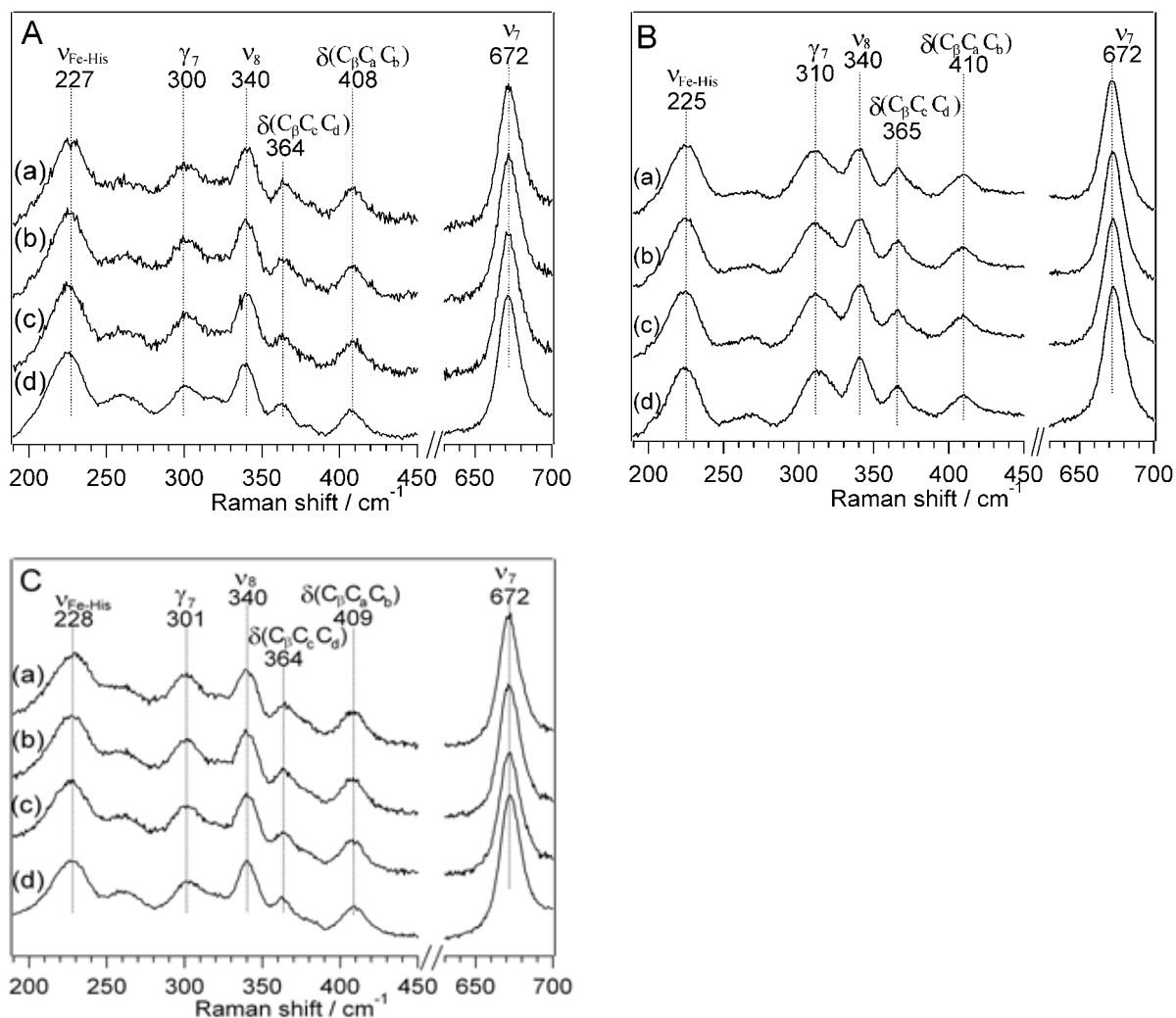
Figure 2. Resonance Raman spectra of (A) full-length WT, (B) full-length Y133F, and (C) the sensor domain of WT. (a)-(c): TR3 spectra of the products of CO-photodissociation for a 10 ps, 100 ps, and 1000 ps delay, respectively. (d): resonance Raman spectra of the deoxy form. These spectra are normalized using the intensity of ν_7 bands.

The ν_{Fe-His} band of WT HemAT-Bs

The ν_{Fe-His} band exhibited a time-dependent change in the intensity and frequency suggesting a structural relaxation following the CO-photodissociation. The intensity of the ν_{Fe-His}

band for the 10 ps photoproduct was smaller than that of the deoxy form, while the intensity of this band for the 100 ps photoproduct became equal to that of the deoxy form (Figure 3A a,b). A similar behavior in the intensity change is reported even in a heme model compound without protein matrix,[10] suggesting that this intensity change occurs independently from the protein conformational change.

The change in the frequency of the ν_{Fe-His} band in WT upon photolysis proceeded more slowly than the change in the intensity did. The ν_{Fe-His} band of the 10 ps photoproduct was observed at a higher frequency by about 2 cm^{-1} compared with that of the deoxy form (225 cm^{-1}), but the frequency difference is too small to evaluate the time-course of the frequency shift precisely. The author therefore uses the difference spectra of the photoproducts vs. the deoxy form, where a ν_{Fe-His} frequency difference gives a peak and trough in the difference spectrum. The 10 ps and 100 ps photoproducts gave the difference spectra with a peak at higher-frequency and a trough at lower-frequency (Figure 3A d,e), indicating that these photoproducts give higher ν_{Fe-His} frequencies than the deoxy form does. This peak and trough finally disappeared in the difference spectrum of the 1000 ps photoproduct (Figure 3A f), representing that the ν_{Fe-His} frequency became identical to that of the deoxy form. Such a frequency shift is not observed in the heme model compound.[10] Therefore, this frequency shift can be judged to correlate to a protein conformational change.

There are three possible causes for the change in the ν_{Fe-His} peak: (1) an out-of-plane displacement of the heme-iron, (2) an alteration of tilt and/or azimuthal angle of the proximal His, and (3) a change of hydrogen bond to the proximal His. The factors (1) and (2) also lead to an intensity change of the ν_{Fe-His} band by the alteration of the overlapping of the σ^*_{Fe-His} orbital and the $\pi^*_{porphyrin}$ orbital, whereas the factor (3) does not cause the intensity change.[10] The ν_{Fe-His} frequency alteration in WT HemAT-Bs would be therefore mainly caused by a change of the hydrogen bond to His123.

In general, a hydrogen bond to the proximal His increases the basicity of the imidazole ring of the proximal His residue, resulting in the strengthening of the Fe—His bond. Consequently, the hydrogen bond to the proximal His makes the ν_{Fe-His} frequency higher. Given that the photoproduct immediately after photolysis retains the proximal interaction of the ligand-bound form, the change in

the $\nu_{Fe\text{—}His}$ frequency upon photolysis in HemAT-Bs reveals a stronger hydrogen bond to the proximal His in the CO-bound form compared with the deoxy form.

The $\nu_{Fe\text{—}His}$ band of Y133F HemAT-Bs

The intensity of the $\nu_{Fe\text{—}His}$ band for the 10 ps photoproduct was smaller than that of the deoxy form in Y133F mutant, while the intensity of this band for the 100 ps photoproduct became equal to that of the deoxy form, as is the case of WT (Figure 3A a,b). Whereas the time-course of the frequency alteration in the $\nu_{Fe\text{—}His}$ band of Y133F proceeded in a different pattern from that of WT. In the case of Y133F mutant, the $\nu_{Fe\text{—}His}$ band for the 10 ps photoproduct was observed at very close frequency to that of the deoxy form (224 cm^{-1}), which gave a much smaller peak and trough in the difference spectrum compared with that of WT (Figure 3B d). For the 100 ps photoproduct, the $\nu_{Fe\text{—}His}$ band already became identical to that of the deoxy form, showing no peak and trough in the difference spectrum (Figure 3B b, e). Thus, unlike the case of WT, the substantial $\nu_{Fe\text{—}His}$ frequency shift upon photolysis was not observed in Y133F mutant. These results indicate that Tyr133 is the partner of His123 to form the hydrogen bond.

The $\nu_{Fe\text{—}His}$ band of the sensor domain of WT HemAT-Bs

In the spectra for the sensor domain of WT, the frequency alteration of the $\nu_{Fe\text{—}His}$ band was smaller than that of the full-length WT, and was completely relaxed within 100 ps (Figure 3C). The $\nu_{Fe\text{—}His}$ intensities for the 100 and 1000 ps photoproducts of the sensor domain were higher than that of the deoxy form, probably because of the alteration in the angular orientation of the proximal His as observed in the reported crystal structure.[3] The pattern of the intensity change and the time-course of the frequency change in the $\nu_{Fe\text{—}His}$ band is disrupted by the deletion of the signaling domain even in the presence of Tyrr133 in the sensor domain, indicating a structural linkage of the proximal heme pocket and the signaling domain. Thus, the hydrogen bond formation between His123 and Tyr133

would play a role for the transmission of a conformational alteration from the heme to the signaling domain.
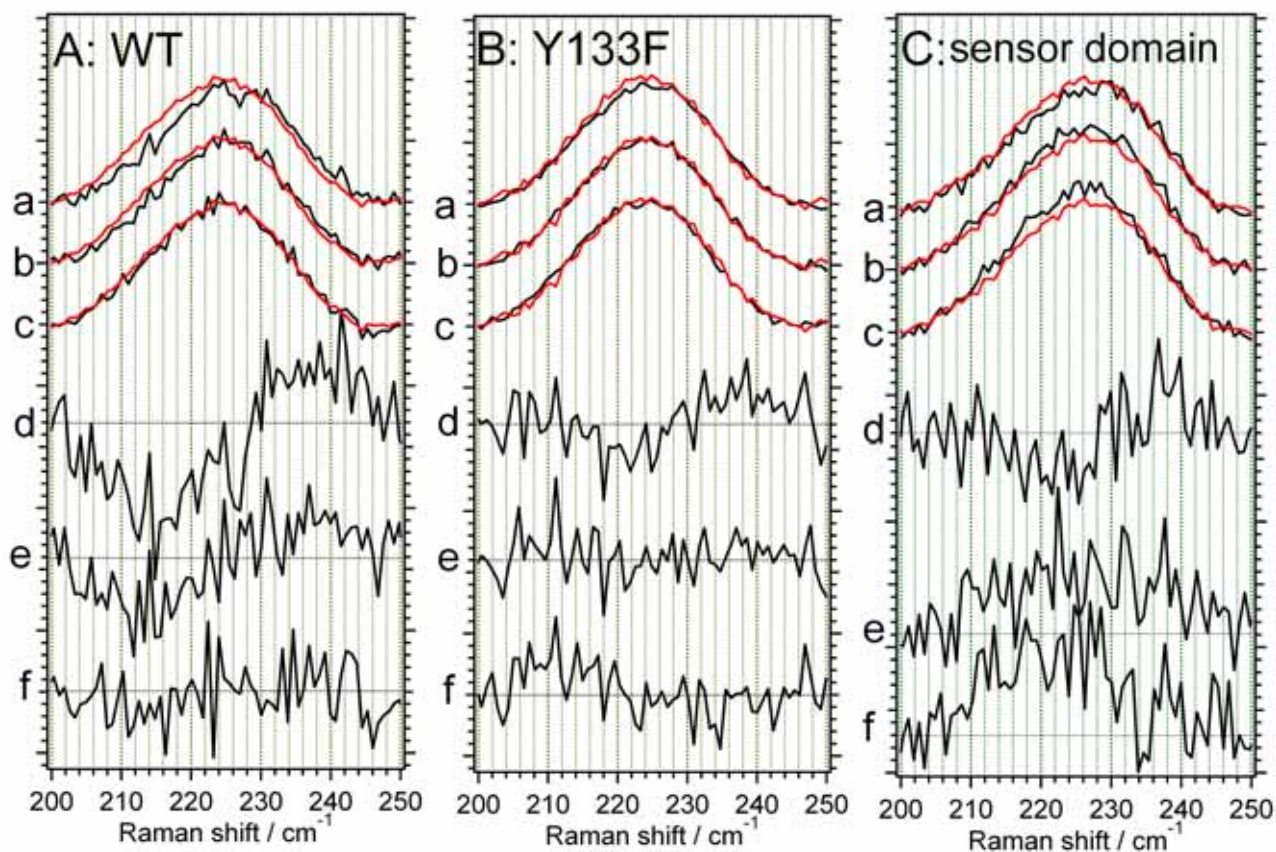

Figure 3. The ν_{Fe-His} band in the TR3 spectra of (A) full-length WT, (B) full-length Y133F, and (C) the sensor domain of WT. The TR3 spectra for the (a) 10ps, (b) 100 ps, and (c) 1000 ps photoproducts are shown as the black lines. The overlapped red lines display the spectra of the deoxy form. The line (d)-(f) exhibit the 5 times enlarged difference spectra of the 10 ps, 100 ps, and 1000 ps photoproduct vs. the deoxy from, respectively. These spectra in the respective panels are normalized using the intensity of ν_7 bands. The intensity for the deoxy forms in WT and Y133F are made to be identical.

Discussion

As described in the result section, the substantial time-dependent frequency shift of the $\nu_{\text{Fe—His}}$ band was observed upon photolysis only in WT. On the other hand, such frequency shift was not observed in Y133F. These results indicate that the $\nu_{\text{Fe—His}}$ frequency shift in WT is caused by the change of a hydrogen bond between Tyr133 and His123, which is induced by the ligand binding/dissociation (Scheme 1). This proximal interaction between His123 and Tyr133 induced by ligand binding would play an important role for signal transduction of HemAT-Bs, as discussed below.

Scheme 1
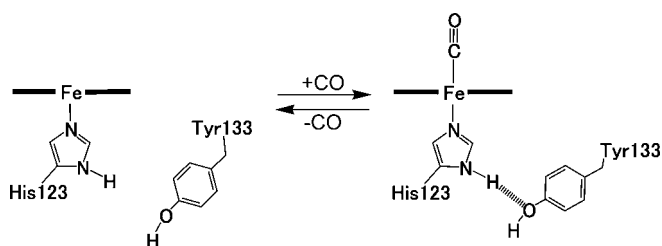
The following mechanism is proposed for the signal transduction in general bacterial chemotactic sensor proteins (MCPs) that are homodimeric membrane-bound proteins. A pair of two antiparallel helices in MCP dimer forms a transmembrane four-helix bundle that connects the periplasmic sensor domain and the cytoplasmic signaling domain. The binding of effector molecule to the sensor domain induces a slide and/or a rotational movement of this helix bundle, which is a key step in the signal transduction of MCPs.[15,16] Although HemAT-Bs is a soluble protein, it is a member of MCPs. Despite lacking of the transmembrane region in HemAT-Bs, two antiparallel helices, the G and H helices, exist in the C-terminal of the sensor domain of HemAT-Bs, and forms a four-helix bundle in the homodimer of HemAT-Bs (Figure 4). The H helix is followed by the

signaling domain. Given that HemAT-Bs adopts the same mechanism for intramolecular signal transduction as do typical membrane-bound MCPs, the helix bundle consisting of the G and H helices will correspond to the transmembrane helix bundle in typical MCPs. Since Tyr133 is located in the G helix, the formation of the hydrogen bond between His123 and Tyr133 would induce a movement of the G helix, and would be a trigger of the signal transduction from the sensor domain to the signaling domain through the movement of the G-H helix bundle.
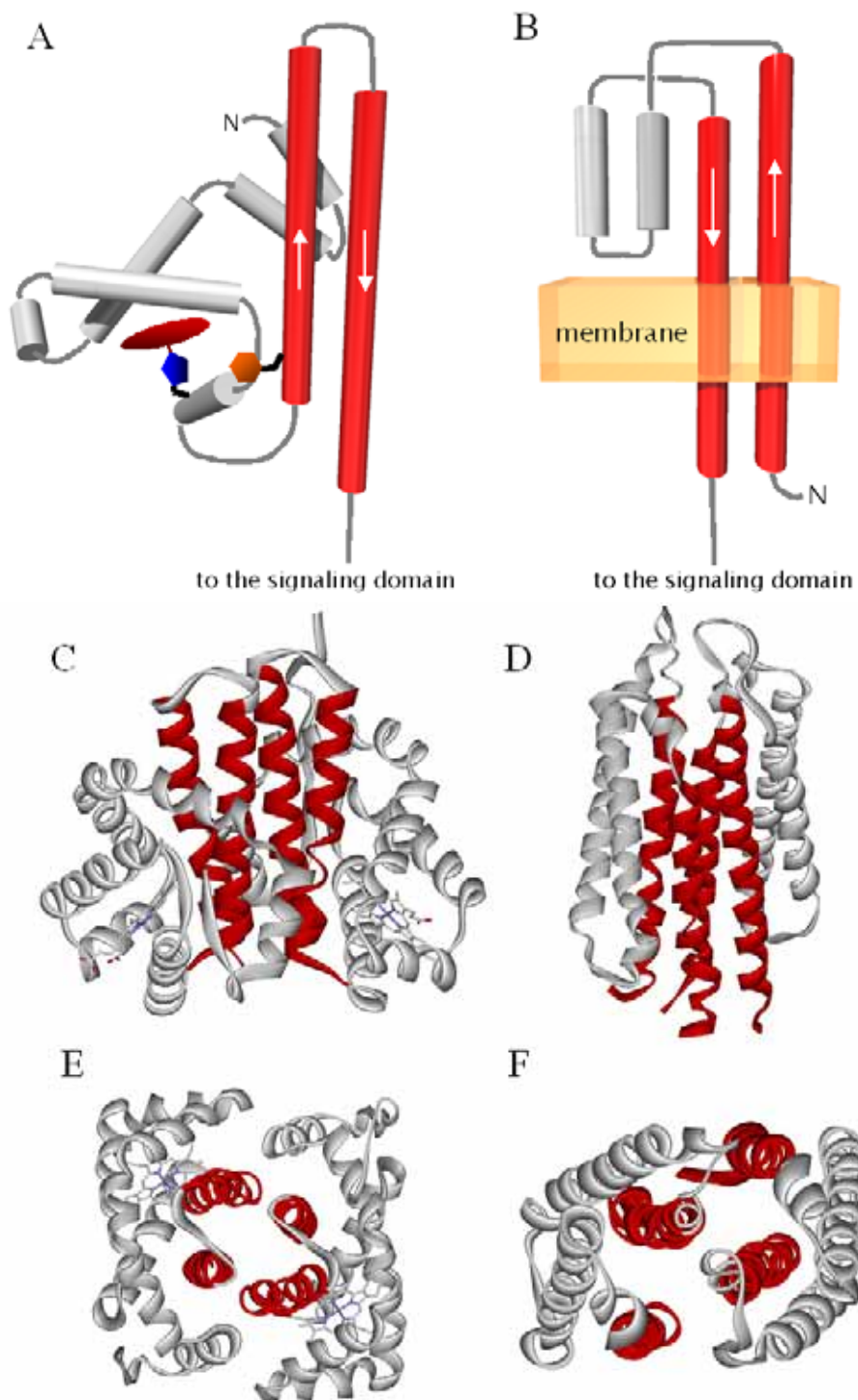
Figure 4. (A), (B): The models of the sensor domain of HemAT-Bs and the sensor and transmembrane domains of MCP, respectively. (C), (D): The crystal structures of sensor domains in HemAT-Bs (1OR6) and Tar from Salmonella (1WAT) that is a typical MCP, respectively. (E), (F): The top view of (C) and (D), respectively. The helices colored red are the constituent of the conserved helix bundle.

Recently, Pinakoulaki et al. have found a ligand accommodation cavity in the protein matrix of HemAT-Bs.[8] The FTIR spectroscopy in the study detects a CO molecule trapped in the protein matrix in the CO-bound WT HemAT-Bs. Mutagenesis and FTIR studies revealed that Tyr133 interacts with the trapped CO. According to these results, this ligand accommodation cavity in HemAT-Bs is proposed to be involved in the signal transduction and/or the regulation of the affinity for the ligand binding to the heme. The movement of Tyr133 upon ligand binding would also affect the physiological function of this cavity.

The important point to discuss about the signaling through the proximal pathway in HemAT-Bs is whether the magnitude of this structural alteration in the heme proximal pocket upon ligand binding is enough for the signal transduction. To discuss about this issue, the case of Mb is instructive, partly because HemAT-Bs sensor domain and Mb are the member of globin sharing a structural homology.

The $\nu_{Fe—His}$ frequency of the CO-bound Mb exhibits 2 cm^{-1} downshift upon photodissociation of CO in hundreds ps by the alteration of the hydrogen bond on the proximal His, relaxing to the identical spectra of the deoxy Mb.[10] Because this phenomenon is very similar to that of HemAT-Bs, the conformational alteration in the heme proximal pocket in Mb and HemAT-Bs would very close in the pattern and the magnitude.

Another report on UV resonance Raman spectroscopic study on Mb shows that binding of CO, NO, and O_2 to the heme causes the conformational change in both the N- and the C-terminal regions.[17,18] Furthermore the hydrogen-bonding network in the heme proximal side of Mb is essential to induce this protein conformational alteration.[16] Therefore, the proximal conformation change in HemAT-Bs can cause a structural alteration of the protein moiety. Thus the conformational alteration of heme proximal pocket in HemAT-Bs would be possible to induce the protein conformational change to induce the signaling event.

The hydrogen-bond formation in the proximal heme pocket of HemAT-Bs upon ligand binding is unprecedented mechanism for the signal transduction in heme proteins, although two examples are reported for the signaling transduction through the heme proximal pocket to date.

One is the case of soluble guanylate cyclase, sGC, which is a heme-based NO sensor protein.[19] The enzymatic activity of guanylate cyclase is activated by NO binding to the heme in sGC. When NO binds to the heme in sGC, the proximal His is dissociated from the heme, resulting in the formation of a 5-coordinated NO-bound heme (Figure 5).[19] Upon binding of CO, the proximal His is not dissociated, and a 6-coordinated heme is formed in sGC, by which sGC is not activated. In this case, the dissociation of the proximal ligand from the heme upon the ligand binding to the trans position is a trigger of the signal transduction through the proximal heme pocket.
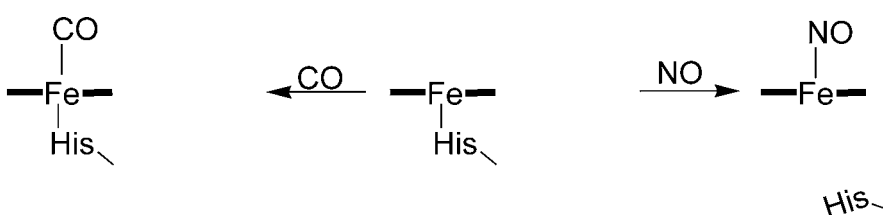
Figure 5. The pattern of conformational alteration in sGC upon CO or NO binding.

The other example is the case of hemoglobin (Hb), where the binding of a ligand induces an in-plane movement of the heme iron, resulting in an allosteric R-T transition through the interaction between the heme and the proximal His (Figure 6).[20] The R-T transition involves the change in constraint on the proximal His by the F-helix imposed by intersubunit interactions. As the result of this constraint, the $v_{Fe—His}$ band of the human HbA CO-photoproduct was observed at higher frequency by 15 cm^{-1} compared with that of the equilibrium deoxy form (214 cm^{-1}), and downshifts to 214 cm^{-1} in tens of
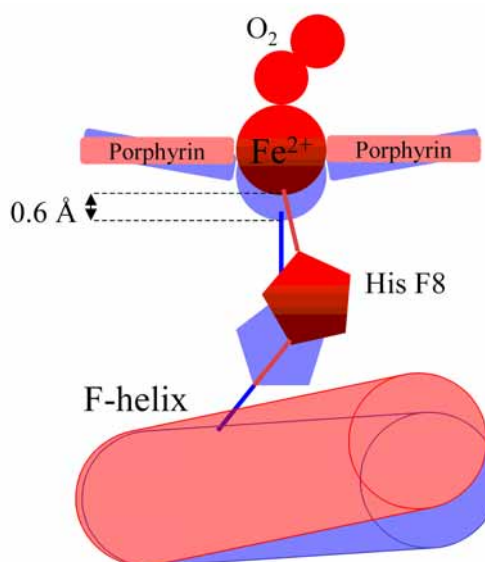

Figure 6. The conformational alteration in the proximal heme pocket in Hb upon ligand binding.

$\mu s,$[21,22] which is a completely different pattern from the case of HemAT-Bs. Thus HemAT-Bs delineate a new mechanism in heme proteins by which the signal transduction is triggered by the formation of the hydrogen bond in the proximal heme pocket upon ligand binding.

The putative signal transduction pathway is present not only through the proximal heme pocket, but also through the distal heme pocket. In the case of HemAT-Bs, the hydrogen bond formation between His86 and the heme propionate, and between Thr95 and heme-bound O_2 would induce the substantial conformational change in the neighboring protein structure. As mentioned in the Chapter 2, this conformational change may be transmitted to the protein matrix through the interaction between Tyr70 in the B helix and Leu92 in the E helix. The B helix is positioned next to the G helix. Therefore, the conformational alteration in the distal heme pocket may also affect the movement of the G helix. Thus, HemAT-Bs would utilize both of the distal and the proximal pathways to introduce the signaling event.

Although there is no absolute explanation for the reason for that HemAT-Bs utilizes two pathways for the signal transduction, the author supposes one possibility for the reason. In the case of CooA and sGC, the signal transduction is induced by ligand exchange or dissociation of internal axial ligand. Such mechanisms with alteration of the coordination structure would be reliable for introducing the protein conformational alteration. On the other hand, both of the distal and the proximal pathway in HemAT-Bs consist of the alteration of hydrogen-bonding networks. A hydrogen bond is one of weak interaction and uncertain to induce a substantial conformational change of the protein matrix. In HemAT-Bs, the distal pathway would more important than the proximal tpathway because only the distal heme pocket can discriminate O_2 from other ligands. Accordingly, HemAT-Bs may utilize the proximal pathway to support the distal pathway.

REFERENCES

1. Hou, S., Larsen, R. W., Boudko, F., Riley, C. W., Karatan, E., Zimmer, M., Ordal, G. W. and Alam, M. (2000) Myoglobin-like aerotaxis transducers in Archaea and Bacteria, *Nature 403*, 540-544

2. Aono, S., Kato, T., Matsuki, M., Nakajima, H., Ohta, T., Uchida, T., and Kitagawa, T., (2002) Resonance Raman and ligand binding studies of the oxygen-sensing signal transducer protein HemAT from *Bacillus subtilis*, *J. Biol. Chem. 277,* 13528-13538

3. Zhang, W. and Phillips, G. N. Jr. (2003) Structure of the oxygen sensor in *Bacillus subtilis*: signal transduction of chemotaxis by control of symmetry, *Structure 11*, 1097-1110

4. Ohta, T., Yoshimura, H., Yoshioka, S., Aono, S. and Kitagawa, T. (2004) Oxygen-sensing mechanism of HemAT from *Bacillus subtilis*: A resonance Raman spectroscopic study, *J. Am. Chem. Soc. 126*, 15000-15001

5. Zhang, W., Olson, J. S. and Phillips, G. N. Jr. (2005) Biophysical and kinetic characterization of HemAT, an aerotaxis receptor from *Bacillus subtilis*, *Biophys. J. 88*, 2801-2814

6. Pinakoulaki, E., Yoshimura, H., Yoshioka, S., Aono, S. and Varotsis, C. (2006) Recognition and discrimination of gases by the oxygen-sensing signal transducer protein HemAT as revealed by FTIR spectroscopy, *Biochemistry 45*, 7763-7766

7. Yoshimura, H., Yoshioka, S., Kobayashi, K., Ohta, T., Uchida, T., Kubo, M., Kitagawa, T., and Aono, S. (2006) Specific hydrogen-bonding networks responsible for selective O_2 sensing of the oxygen sensor protein HemAT from *Bacillus subtilis*, *Biochemistry 45*, 8301-8307

8. Pinakoulaki, E., Yoshimura, H., Daskalakis, V., Yoshioka, S., Aono, S. and Varotsis, C. (2006) Two ligand binding sites in the O_2-sensing signal transducer HemAT: implication for ligand recognition/discrimination and signaling, *Proc. Natl. Acad. Sci. USA 103*, 14794-14801

9. Uchida, T., Kitagawa, T. (2005) Mechanism for transduction of the ligand-binding signal in heme-based gas sensory proteins revealed by resonance Raman spectroscopy, *Acc. Chem. Res. 38*,

662-670

10.   Mizutani, Y. and Kitagawa, T. (2001) Ultrafast structural relaxation of myoglobin following photodissociation of carbon monoxide probed by time-resolved resonance Raman spectroscopy, *J. Phys. Chem. B* 105, 10992-10999

11.   Kitagawa, T., Haruta, N. and Mizutani, T. (2002) Time-resolved resonance Raman study on Ultrafast structural relaxation and vibrational cooling of photodissociated carbonmonoxy myoglobin, *Biopolymers, 67*, 207-213

12.   Mizutani, Y. and Kitagawa, T. (2001) Ultrafast dynamics of myoglobin probed by time-resolved resonance Raman spectroscopy, *Chem. Rec., 1*, 258-275

13.   Hu, S., Smith, K. M. and Spiro, T. G. (1996) Assignment of protoheme resonance Raman spectrum by heme labeling in myoglobin, *J. Am. Chem. Soc., 118*, 12638-12646

14.   Peterson, E. S., Friedman, J. M., Chien, E. Y. T. and Sligar, S. G. (1998) Functional implication of the proximal hydrogen-bonding network in myoglobin: a resonance Raman and kinetic study of Leu89, Ser92, His97, and F-helix swap mutants, *Biochemistry 37*, 12301-12319

15.   Ottemann, K. M., Xiao, W., Shin, Y. and Koshland, D. E. Jr. (1999) A piston model for transmembrane signaling of the aspartate receptor, *Science, 285*, 1751-1754

16.   Szurmant, H., Bunn, M. W., Cho, S. H. and Ordal, G. W. (2004) Ligand-induced conformational changes in the *Bacillus subtilis* chemoreceptor McpB determined by disulfide crosslinking *in vivo*, *J. Mol. Biol., 344*, 919-928

17.   Sato, S. and Mizutani, Y. (2005) Picosecond structural dynamics of myoglobin following photodissociation of carbon monoxide as reveald by ultraviolet time-resolved resonance Raman spectroscopy, *Biochemistry, 44*, 14709-14714

18.   Gao, Y., El-Mashtoly, S. F., Pal, B., Hayashi, T., Harada, K. and Kitagawa, T. (2006) Pathway of information transmission from heme to protein upon ligand binding/dissociation in myoglobin revealed by UV resonance Raman spectroscopy, *J. Biol. Chem., 281*, 24637-24646

19.   Pal, B. and Kitagawa, T. (2005) Interactions of soluble guanylate cyclase with diatomics as probed by resonance Raman spectroscopy, *J. Inorg. Biochem.*, *99*, 267-279

20.   Perutz, M. F. (1970) Stereochemistry of cooperative effects in haemoglobin: haem−haem interaction and the problem of allostery, *Nature*, *228*, 726-739

21.   Samuni, U., Ouellet, Y., Guertin, M., Friedman, J. M. and Yeh, S (2004) The absence of proximal strain in the truncated hemoglobins from *Mycobacterium tuberculosis*, *J. Am. Chem. Soc.*, *126*, 2682-2683

22.   Scott, T. W. and Friedman, J. M. (1984) Tertiary-structure relaxation in hemoglobin: a transient Raman study, *J. Am. Chem. Soc.*, *106*, 5677-5687

Chapter 4: Summary and Future Perspectives

In this thesis, the author aimed to reveal the molecular mechanism of the selective O_2 sensing and the signal transduction in HemAT-Bs. For this purpose, the author utilized a variety of spectroscopic method including resonance Raman, EPR, and UV-Vis spectroscopies with mutagenesis studies.

The author studied the mechanism of the selective O_2 sensing by HemAT-Bs in the Chapter 2. The resonance Raman spectroscopy revealed that the hydrogen bond between Thr95 and the heme-bound ligand is present only in the O_2-bound form, but not exist in CO- and NO-bound forms. These results indicate that the hydrogen bond between Thr95 and the heme-bound O_2 is essential for O_2 sensing. In addition, the author found that a hydrogen bond to heme propionate exists only in O_2 bound form. With several mutants of the amino acid residues around the heme propionate, the author identified the partner of this hydrogen bond is His86. In O_2-bound HemAT-Bs H86A mutant, the conformer with a direct hydrogen bond between Thr95 and the heme bound O_2, named open α form, disappeared. According to these results, the author proposed the selective O_2 sensing mechanism as follows. The binding of O_2 to the heme in HemAT-Bs induces the hydrogen bond formation between the heme propionate and His86, accompanied by a conformational alteration of the distal heme pocket. As the result of this conformational alteration, Thr95 moves near to the heme-bound O_2 and forms a direct hydrogen bond to the O_2. In the case of the CO- and NO- bound forms, His86 does not form the hydrogen bond to the heme propionate. The absence of the hydrogen bond formation between them will make Thr95 kept too far to form a hydrogen bond to the heme-bound CO and NO. This cascade of hydrogen-bonding formation would be essential for the discrimination of O_2 from CO and NO by HemAT-Bs. In addition, this event would induce a considerable conformational alteration of the protein matrix around the heme, and therefore would be important to induce the signaling event.

Such a mechanism with utilizing a hydrogen bond to the heme propionate is also observed in FixL, another heme-based O_2 sensor protein. As mentioned in Chapter 1, in the case of FixL, Arg220

forms hydrogen bond to the heme-bound ligand only in the O_2-bound form. The reconstruction of the hydrogen bond network takes place only upon O_2 binding, not upon CO and NO binding. These facts suggest that it would be a common principal for heme-based O_2 sensor proteins to utilize not only the specific interaction between the heme-bound O_2 and surrounding amino acid residues in the distal heme pocket, but also the heme propionate for their selective O_2 sensing.

In the Chapter 3, the author showed the hydrogen-bond formation between His123 and Tyr133 upon ligand binding by the measurement of TR3 spectra of WT and Y133F mutant in the deoxy form and the products after photolysis of the CO-bound form. This result is consistent with the reported crystal structure of HemAT-Bs sensor domain where the distance between Tyr133 and the proximal His, His123, is shorter in the CN-bound form than in the deoxy form. The interaction between the heme-bound O_2 and the amino acid residue in the distal heme pocket have been intensively investigated, because it is considered that the specific and direct interaction between the O_2 and the amino acid residue is essential for selective O_2 sensing. However, the interaction between the heme and the proximal heme pocket has not been paid so much attention in heme-based O_2 sensor proteins. The results described in the Chapter 3 suggest the possibility of the signaling pathway through the proximal heme pocket in the heme-based O_2 sensor proteins. Moreover, the mechanism of the signal transduction through the proximal heme pocket in HemAT-Bs is a new mechanism for signal transduction in heme proteins.

Although these results give much information to understand the general and novel mechanisms of selective O_2 sensing by heme-based O_2 sensor proteins and of induction of the signaling, even some issues remains unclear. First, there is no direct evidence of the involvement of hydrogen bonding between for the physiological function of HemAT-Bs. The author tried to prepare the *in vitro* assay system to measure HemAT-Bs activity by constructing the HemAT-CheA-CheW complex. However, the complex formation by mixing of these proteins *in vitro* was not succeed because of aggregation of the Che proteins, especially that of CheW. To avoid the aggregation of Che proteins, it would be effective to use the co-expression system for HemAT-Bs, CheA, and CheW under controlling the expression level of each protein. With this co-expression system, the complex formed in *E. coli* cells could be purified.

Moreover, the physiological role of the three conformers present in the O_2-bound HemAT is unclear. One of the plausible possibilities for the reason of the existence of the three conformers is that the multi-conformer reflects the cooperativity or the difference of the ligand binding affinity between the two subunit. In fact, MCPs generally display a negative cooperativity of the ligand binding affinity. The measurement of HemAT-Bs activity in different O_2 partial pressure is required to confirm if this is the case.

Another issue remains to be studied is to analyze the conformational alteration of HemAT-Bs upon O_2 binding. The physiological function of HemAT-Bs is expressed not only by the heme and surrounding structure, but also the structural alteration of whole protein matrix. The author is now trying to evaluate the conformational change in HemAT-Bs by FRET analysis.

List of Publications

Oxygen-Sensing Mechanism of HemAT from *Bacillus subtilis*: A Resonance Raman Spectroscopic Study

Takehiro Ohta, Hideaki Yoshimura, Shiro Yoshioka, Shigetoshi Aono, and Teizo Kitagawa

J. Am. Chem. Soc., **126**, 15000 -15001, 2004

Biophysical properties of a c-type heme in chemotaxis signal transducer protein DcrA

Shiro Yoshioka, Katsuaki Kobayashi, Hideaki Yoshimura, Takeshi Uchida, Teizo Kitagawa, Shigetoshi Aono

Biochemistry, **44**, 15406-15413, 2005

Non-covalent modification of the heme-pocket of apomyoglobin by a 1,10-phenanthroline derivative

Yutaka Hitomi, Hidefumi Mukai, Hideaki Yoshimura, Tsunehiro Tanaka and Takuzo Funabiki
Bioorganic & Medicinal Chemistry Letters, **16**, 248-251, 2006

Recognition and discrimination of gases by the oxygen-sensing signal transducer protein HemAT as revealed by FTIR spectroscopy

Eftychia Pinakoulaki, Hideaki Yoshimura, Shiro Yoshioka, Shigetoshi Aono, Constantinos Varotsis
Biochemistry, **45,** 7763-7766, 2006

Specific hydrogen-bonding networks responsible for selective O_2 sensing of the oxygen sensor protein HemAT from *Bacillus subtilis*

Hideaki Yoshimura, Shiro Yoshioka, Katsuaki Kobayashi, Takehiro Ohta, Takeshi Uchida, Minoru Kubo, Teizo Kitagawa, Shigetoshi Aono
Biochemistry, **45,** 8301-8307, 2006

Two ligand-binding sites in the O$_2$-sensing signal transducer HemAT: Implications for ligand recognition/discrimination and signaling

Eftychia Pinakoulaki, Hideaki Yoshimura, Vangelis Daskalakis, Shiro Yoshioka, Shigetoshi Aono, Constantinos Varotsis

The Signal Transduction Mechanism of HemAT-Bs through the proximal heme pocket Revealed by Time-resolved Resonance Raman Spectroscopy

Hideaki Yoshimura, Shiro Yoshioka, Yasuhisa Mizutani, Shigetoshi Aono

Acknowledgements

January 2007

Okazaki

Hideaki Yoshimura